

REPORT DOCUMENTATION PAGE			Form Approved OMB No. 0704-0180	
Public reporting burden for this collection of information is estimated to average 1 hour per response, including the time for reviewing the data needed, and completing and reviewing the collection of information. Send comments regarding this burden estimate or any other aspect of this collection of information, including suggestions for reducing this burden, to Washington Headquarters Services, Directorate for Information Operations and Reports, 1204, Arlington, VA 22202-4302, and to the Office of Management and Budget, Paperwork Reduction Project (0704-0180).				
1. AGENCY USE ONLY (Leave Blank)	2. REPORT DATE	3. REPORT TYPE	AFRL-SR-BL-TR-98-	
13	March 1995	Final	0442	
4. TITLE AND SUBTITLE			5. FUNDING NUMBERS	
Cleavage Mapping the Topology of Protein Folding Intermediates				
6. AUTHORS				
David W. Ledman				
7. PERFORMING ORGANIZATION NAME(S) AND ADDRESS(ES)			8. PERFORMING ORGANIZATION REPORT NUMBER	
Yale University				
9. SPONSORING/MONITORING AGENCY NAME(S) AND ADDRESS(ES)			10. SPONSORING/MONITORING AGENCY REPORT NUMBER	
AFOSR/NI 110 Duncan Avenue, Room B-115 Bolling Air Force Base, DC 20332-8080				
11. SUPPLEMENTARY NOTES				
12a. DISTRIBUTION AVAILABILITY STATEMENT			12b. DISTRIBUTION CODE	
Approved for Public Release				
13. ABSTRACT (Maximum 200 words)				
See attached.				
<div style="border: 1px solid black; padding: 5px; display: inline-block;"> <b>DISTRIBUTION STATEMENT A</b>            Approved for public release            Distribution unlimited         </div>				
14. SUBJECT TERMS			15. NUMBER OF PAGES	
			16. PRICE CODE	
17. SECURITY CLASSIFICATION OF REPORT	18. SECURITY CLASSIFICATION OF THIS PAGE	19. SECURITY CLASSIFICATION OF ABSTRACT	20. LIMITATION OF ABSTRACT	
Unclassified	Unclassified	Unclassified	UL	

19980518 022

DTIC QUALITY INSPECTED 5

In order to identify regions of the polypeptide chain that are brought close together by the protein fold, our laboratory devised a scheme in which, in the presence of reductant, reactive oxygen species are generated at an EDTA-Fe moiety covalently attached to unique cysteine residues in a series of single cysteine mutants of the protein under study. Only surface residues that do not participate in side chain interactions are mutated. The mutants undergo a thiol exchange reaction in the presence of EPD-Fe that results in the attachment of the EDTA-Fe moiety. The free radicals generated at the iron center promote intramolecular, conformation dependent cleavage of the peptide backbone. This procedure applied to folded and unfolded staphylococcal nuclease, for which the crystal structure is solved at high resolution, showed that the reaction is dependent on the distance between the cleavage site and the EDTA-Fe moiety as well as accessibility to the reactive oxygen species generated at the iron center (1 and 2). The sites of cleavage are identified using SDS-PAGE, HPLC, protein sequencing, and mass spectrometry.

Cleavage sites identified in the folded full length protein serve as markers to identify regions of the protein that are interacting under nonnative conditions. The above strategy has been applied to the 1-135 fragment (out of 149) of staphylococcal nuclease. Large N-terminal fragments of staphylococcal nuclease are compact but have only a low level of secondary structure as measured by circular dichroism spectroscopy (3 and 4). These fragments lack only six residues that are ordered in the crystal structure, and retain near wild-type catalytic activity. Upon the addition of the ligands calcium and pdTp, they fold with concomitant restoration of spectral properties. When the fragments are incubated with calcium and pdTp and then subjected to cleavage, cleavage patterns and sites are identified that show long range interactions and strongly support a native-like fold. Without these ligands cleavage sites are identified that support the integrity of the  $\beta$ -barrel, and others show that the loop between helices 2 and 3 is disordered and that helix 3 is melted away from the globular remainder of the protein (Ermácora et al., in preparation).

Certain mutations have a profound effect on the stability of the folded state of nuclease. The cleavage technique will be used to investigate the changes that occur in two of these mutants. V66L has a greatly lowered  $m$  value while that of A90S is substantially increased (5). Cysteine mutants at position 11, 64, and 124 have been used to monitor the integrity of the beta sheet and association of the three helices. Attachment of the reagent at residue 16 is predicted to yield cleavages that monitor the association of helix one with the beta sheet while attachment at position 30 is predicted to yield cleavages that monitor other interactions within the beta barrel. CD spectra and unfolding curves of these modified proteins will be used to determine if they are suitable. If they are suitable, these mutants will be generated in the fragment contexts and used with the other mutants to determine the effect of the  $m$  value mutations on the topology of this model folding intermediate. Otherwise two new cysteine mutants will be found that meet these criteria. The two new full length cysteine mutants and their 1 - 135 fragments will be subjected to cleavage conditions and the products analyzed by techniques optimized over the last two years. Once the cleavage sites are identified, the  $m^+$  and  $m^-$  mutants will be analyzed at the gel level by comparison to the cleavage patterns for the cysteine mutants without the  $m$ -value mutation. Mutants that give rise to new bands will be characterized in detail by the above procedures as time allows.

This procedure has been applied to the myoglobin molten globule state and has identified near native regions of the protein that have previously been undetected. At the gel level of analysis, the molten globule gives remarkably similar results as the fully folded apoprotein. Detailed characterization is still in progress.

1. Ermácora, M. R., Delfino, J. M., Cuenoud, B., Schepartz, A. & Fox, R. O. (1992) *Proc. Natl. Acad. Sci. USA* 89, 6383 - 6387.
2. Ermácora, M. R., Ledman, D. W., Hellinga, H. W., Hsu, G. W., and Fox, R. O. *Biochemistry*, 33, 1625 - 41.
3. Flanagan, J. M., Kataoka, M., Shortle, D., and Engelman, D. M. (1991) *Proc. Natl. Acad. Sci. USA* 89, 748 - 52.

[illegible]

In order to identify regions of the polypeptide chain that are brought close together by the protein fold, our laboratory devised a scheme in which, in the presence of reductant, reactive oxygen species are generated at an EDTA-Fe moiety covalently attached to unique cysteine residues in a series of single cysteine mutants of the protein under study. Only surface residues that do not participate in side chain interactions are mutated. The mutants undergo a thiol exchange reaction in the presence of EPD-Fe that results in the attachment of the EDTA-Fe moiety. The free radicals generated at the iron center promote intramolecular, conformation dependent cleavage of the peptide backbone. This procedure applied to folded and unfolded staphylococcal nuclease, for which the crystal structure is solved at high resolution, showed that the reaction is dependent on the distance between the cleavage site and the EDTA-Fe moiety as well as accessibility to the reactive oxygen species generated at the iron center (1 and 2). The sites of cleavage are identified using SDS-PAGE, HPLC, protein sequencing, and mass spectrometry.

Cleavage sites identified in the folded full length protein serve as markers to identify regions of the protein that are interacting under nonnative conditions. The above strategy has been applied to the 1-135 fragment (out of 149) of staphylococcal nuclease. Large N-terminal fragments of staphylococcal nuclease are compact but have only a low level of secondary structure as measured by circular dichroism spectroscopy (3 and 4). These fragments lack only six residues that are ordered in the crystal structure, and retain near wild-type catalytic activity. Upon the addition of the ligands calcium and pdTp, they fold with concomitant restoration of spectral properties. When the fragments are incubated with calcium and pdTp and then subjected to cleavage, cleavage patterns and sites are identified that show long range interactions and strongly support a native-like fold. Without these ligands cleavage sites are identified that support the integrity of the  $\beta$ -barrel, and others show that the loop between helices 2 and 3 is disordered and that helix 3 is melted away from the globular remainder of the protein (Ermácora et al., in preparation).

Certain mutations have a profound effect on the stability of the folded state of nuclease. The cleavage technique will be used to investigate the changes that occur in two of these mutants. V66L has a greatly lowered  $m$  value while that of A90S is substantially increased (5). Cysteine mutants at position 11, 64, and 124 have been used to monitor the integrity of the beta sheet and association of the three helices. Attachment of the reagent at residue 16 is predicted to yield cleavages that monitor the association of helix one with the beta sheet while attachment at position 30 is predicted to yield cleavages that monitor other interactions within the beta barrel. CD spectra and unfolding curves of these modified proteins will be used to determine if they are suitable. If they are suitable, these mutants will be generated in the fragment contexts and used with the other mutants to determine the effect of the  $m$  value mutations on the topology of this model folding intermediate. Otherwise two new cysteine mutants will be found that meet these criteria. The two new full length cysteine mutants and their 1 - 135 fragments will be subjected to cleavage conditions and the products analyzed by techniques optimized over the last two years. Once the cleavage sites are identified, the  $m^+$  and  $m^-$  mutants will be analyzed at the gel level by comparison to the cleavage patterns for the cysteine mutants without the  $m$ -value mutation. Mutants that give rise to new bands will be characterized in detail by the above procedures as time allows.

This procedure has been applied to the myoglobin molten globule state and has identified near native regions of the protein that have previously been undetected. At the gel level of analysis, the molten globule gives remarkably similar results as the fully folded apoprotein. Detailed characterization is still in progress.

1. Ermácora, M. R., Delfino, J. M., Cuenoud, B., Schepartz, A. & Fox, R. O. (1992) *Proc. Natl. Acad. Sci. USA* 89, 6383 - 6387.
2. Ermácora, M. R., Ledman, D. W., Hellinga, H. W., Hsu, G. W., and Fox, R. O. *Biochemistry*, 33, 1625 - 41.
3. Flanagan, J. M., Kataoka, M., Shortle, D., and Engelman, D. M. (1991) *Proc. Natl. Acad. Sci. USA* 89, 748 - 52.

4. Shortle, D. and Mecker, A. (1989) *Biochemistry* 28,, 936 - 44.
5. Shortle, D. and Mecker, A. (1986) *Proteins: Structure, Function, and Genetics* 1, 81 - 89.

## Schedule for Completion of Ph.D. Research

Ph.D. awarded December 1996

thesis submitted September 1, 1996

start writing thesis July 1, 1996 - 2 months to complete

finish cleavage and analysis of fragments by the end of June 1996 - 6 months to complete

CD, sizing, and unfolding curves finished by the end of December 1995 - 2 month to complete

protein purification finished by the end of October 1995 - 3 months to complete

finish all cloning by the end of July 1995 - 4 months to complete

# Mapping the structure of a nonnative state of staphylococcal nuclease

Mario R. Ermácora<sup>1, 2, 3</sup>, David W. Ledman<sup>2</sup>, and  
Robert O. Fox<sup>1, 2, 4</sup>

<sup>1</sup>The Howard Hughes Medical Institute, and<sup>2</sup>The Department of Molecular Biophysics and Biochemistry, Yale University, 266 Whitney Avenue, New Haven, Connecticut, 06520

<sup>3</sup>Instituto de Química y Fisicoquímica Biológicas, Facultad de Farmacia y Bioquímica (UBA-CONICET), Buenos Aires, Argentina

<sup>4</sup> Present address: The Department of Human Biological Chemistry and Genetics, The University of Texas Medical Branch, Galveston

Running title: Mapping the structure of a SNase nonnative state

Correspondence should be addressed to R.O.F.

---

Dr. Robert O. Fox, Ph.D.  
University of Texas  
Medical Branch at Galveston  
Department of Human Biological Chemistry and Genetics  
Room 5.138H, M.R.B. Building  
Galveston, TX 77555

Nonnative states of proteins (such as the molten globule) populated by extremes of pH or by mutation or truncation of the protein sequence, are thought to be equilibrium models for kinetic intermediates on the folding pathway. While the global physical properties of these molecules have been well characterized, analysis of their structure by NMR spectroscopy has proven difficult. Here we report the use of a new chemical cleavage technique, based on reactive oxygen species, to map the backbone fold of a truncated form of staphylococcal nuclease in a nonnative state. The fragment adopts a native-like fold, however the technique also reveals regions of nonnative structure.

Efforts to characterize the structure of folding intermediates have been thwarted because most form in milliseconds and are not significantly populated at equilibrium<sup>1</sup>. Nonnative states have been favored over the native state by a number of stratagems, in the hope of populating folding intermediates at equilibrium. Some proteins exhibit well-populated nonnative states in the presence of moderate concentrations of acids, urea or guanidinium chloride, and other have been found to partially unfold after the removal of bound calcium or prosthetic groups<sup>2,3</sup>. These nonnative states share several properties: a radius of gyration intermediate between that of the native and the unfolded states; circular dichroism spectra (CD) indicating the presence of substantial secondary structure; binding of 8-anilino-1-naphthalene sulfonate indicative of exposed hydrophobic patches; and loss of near-UV CD signal indicative of disordered aromatic side chains<sup>3</sup>.

Global properties of nonnative states, such as the molten globule or acid forms, including helix content, compactness, and thermodynamic stability, have been reported for a number of small globular proteins. However, very little is known about their detailed structure, mainly due to their unsuitability for X-ray analysis and the difficulties in their characterization by NMR spectroscopy. Amide proton protection studies of equilibrium molten globules of several proteins have been reported<sup>4-13</sup>. A frequent

finding has been the detection of native-like secondary structure and a pattern of protection that is compatible with a native-like ensemble of secondary structure elements. Stopped-flow measurements indicate that this equilibrium structure is indeed a kinetic folding intermediate in the case of apomyoglobin<sup>14</sup>. These results progressively led to the view that molten globules have at least a partial native-like topology<sup>7,8,13,15-17</sup>. Although, alternative models for the highly compact denatured state as an ensemble of various conformations have been proposed<sup>18</sup>. While NMR spectroscopy has been invaluable in characterizing the structure of the native state of proteins, it has been of more limited success in the detailed direct analysis of molten globule conformations<sup>5,19</sup>. This is due in part to the aggregation of samples, dynamic of the molecules leading to resonance broadening, and a lack of sufficient chemical shift dispersion<sup>20</sup>.

We developed a new structural mapping procedure to characterize the conformation of nonnative protein states to complement NMR analysis. Our method is based on the conformation dependent chemical cleavage of the polypeptide chain by reactive oxygen species generated at a cysteine specific tethered EDTA-Fe reagent<sup>21,22</sup>. This procedure, described in Fig. 1, was first tested with several genetically engineered variants of staphylococcal nuclease (SNase)<sup>23</sup>. In these proteins, single cysteine substitutions were introduced at surface residues, and an EDTA-Fe complex was attached specifically to the thiol group. The resulting structures were unperturbed or modestly destabilized. In all cases full enzymatic activity was retained and the conformation was native as judged by CD spectroscopy. Upon incubation of the conjugates with ascorbate, reactive oxygen species were produced that cleaved the polypeptide backbone, with single hit kinetics, in proximity of the attached reagent. In all cases the cleavage occurred at surface accessible sites, either distant in sequence but close in the three-dimensional structure of the protein or contiguous in sequence with the cysteine bearing the EDTA-Fe group. A conformational analysis revealed that the chemical cleavage faithfully mapped the tertiary fold of native staphylococcal nuclease at solvent accessible sites within 5-15

Å of the EPD-Fe modified cysteine<sup>23</sup>. The yield of specific cleavage products also provided a faithful representation of the native population at equilibrium in GuHCl unfolding experiments, presumably by virtue of the short lifetime of the reactive oxygen species involved<sup>23</sup>. Thus, the chemical cleavage method provides information concerning the proximity of secondary structural elements and the surface accessibility of the cleavage sites. Further, the relative cleavage yield can be used to characterize the population of a protein state. Herein we present the first use of the EPD-Fe reagent to characterize the structure of a nonnative state, SNase 1-135, a C-terminal truncated form of SNase (lacking the last 14 of its 149 residues) that acquires a compact state with most of the features of a molten globule.

### **SNase fragments as a model for the partially folded state**

SNase folds efficiently and reversibly and it has no cysteine or prosthetic groups. Compared with the wild type protein, SNase variants in which one or more residues have been mutated show altered values of  $m$ , the dependence of  $\Delta G$  of unfolding on the denaturant concentration<sup>24</sup>. It has been proposed that variants with increased  $m$  values ( $m+$ ) have a more expanded and disordered denatured state while variants with decreased  $m$  values ( $m-$ ) are more compact and ordered under the same conditions. These observations were initially ascribed to residual intramolecular interactions in the denatured states that could be modulated by site-specific mutations<sup>24</sup>. Recently, differential scanning calorimetry studies at low pH showed that the  $m$  value behavior may be due to a change in the population of an intermediate at equilibrium in a three state unfolding mechanism<sup>25</sup>.

The removal of a short stretch of residues from the C-terminus of SNase produces a compact nonnative state in absence of any added denaturant, retaining a fraction of the SNase secondary structure and enzymatic activity. The degree of compactness, as well as the  $\alpha$ -helix content and enzymatic activity can be altered by changing the number of residues deleted. Two SNase ligands,  $\text{Ca}^{2+}$  and  $\text{pdTp}$ , shift SNase fragments toward the

native state. These ligands transform the partially folded state of SNase1-136 into a structure that is indistinguishable from the native state as judged by NMR spectroscopy, X-ray solution scattering, and CD spectroscopy<sup>26,27</sup>. Careful measurements of the temperature and pH dependence of the radius of gyration ( $R_g$ ) and CD spectra, as well as the measurement of the affinity for  $\text{Ca}^{2+}$  and pdTp of these fragments indicate that their intermediate conformational properties are not the result of averaging fully unfolded and fully folded protein at equilibrium. The same conclusion is reached upon examination of NMR spectra of SNase-1-136 in the absence of ligands which gave no indication of native signals even though some residual structure must be present<sup>27</sup>.

C-terminal truncated SNases are extremely attractive as protein folding models because there is no need to use denaturants or harsh conditions to populate a partially folded state. Indeed, the partially folded state produced by C-terminal truncation seems to be a much better approximation to the small population of unfolded or partially folded molecules that co-exist physiologically at equilibrium with the native state than those produced by denaturants<sup>26-28</sup>.

#### **SNase1-135-EDTA-Fe variants have the conformational features of the SNase1-136 system**

No significant perturbation of the enzymatic activity, conformation (as monitored by CD), or thermodynamic stability was observed for the full-length nuclease EPD-Fe-modified variants examined earlier<sup>23</sup>; however, any chemical approach to protein analysis has the potential disadvantage that it may perturb the system under investigation. In addition, the compactness or conformational ensemble of the related SNase1-136 fragment is sensitive to single amino acid substitutions, usually within the core of the protein (see above). Therefore, we carefully examined the physical properties of the EPD-Fe modified and unmodified SNase1-135 single cysteine variants used in the cleavage studies, to ensure that they were comparable to the SNase 1-136 model.

The Stokes radii ( $R_S$ ) of the nuclease fragments and their corresponding EPD-Fe derivatives ranged from 21.6 to 22.0 Å (Fig. 2a). These values compare favorably with the reported  $R_S$  and  $R_g$  of wild type SNase1-136 (22.0 and 21.2 Å respectively)<sup>26-28</sup>. Thus, SNase 1-135 variants are monomeric and almost as compact as full-length native nuclease. The observed variation in  $R_g$  determined by small angle X-ray scattering for various SNase1-136  $m$  value variants<sup>28</sup> ( $m^-$ :  $R_g$ =17.3 to 18.0 Å and  $m^+$ :  $R_g$ =25.0 to 37.0 Å) is much greater than that seen for the  $R_S$  values of the modified cysteine variants examined herein. These results indicate that the cysteine substitution and subsequent EPD-Fe modification do not significantly perturb the conformational manifold of the SNase1-135 fragments.

The EPD-Fe modified SNase1-135 were examined by CD spectroscopy with and without ligands (Fig. 2b). The CD spectra of these fragments were intermediate between the native and random coil spectra as has been observed for SNase1-136. The variation in  $[\theta_{208}]$  and  $[\theta_{222}]$  for the SNase 1-135 cysteine variants is comparable to that seen for several  $m^+$  SNase1-136 variants in the absence of ligands<sup>26-28</sup>. This may indicate that  $\alpha$ -helical structures are less populated in the SNase1-135 cysteine variants used in this study than in the SNase1-136 fragment, although the complete significance of these spectral changes is far from clear. In addition, a native-like state can be favored for all the EPD-Fe modified SNase1-135 cysteine variants on addition of the  $\text{Ca}^{2+}$  and pdTp ligands, as indicated by CD spectra comparable to that reported for the SNase1-136 ligand complex (Fig. 2b). Taken together, the size exclusion and CD results indicate that the cysteine substitution and EPD-Fe modification did not significantly perturb the general conformational features of the SNase fragments. Certainly the system is not biased toward the native state, and the chemical cleavage results reported below for each SNase 1-135 variant may be compared with each other and with the results of previous experiments<sup>23</sup>.

#### EPD-Fe mediated cleavage mapping of SNase1-135

The cleavage reaction of P11C<sub>1-135</sub> and K64C<sub>1-135</sub> resulted in several discrete fragmentation products as shown by SDS-PAGE analysis (Fig. 3a, b; lane 2) that were distinct from those found in the presence of 4.8 M urea where the fragment is largely unfolded (Fig. 3a, b; lane 4). This indicates that persistent and specific long range interactions exist within the fragments. The cleavage pattern of these two variants was largely unaffected by adding Ca<sup>2+</sup> and pdTp, the ligands that promote the native state (Fig. 3a, b; lane 3). This result suggests that the conformation of the fragment mapped by cleavage of these variants is similar to that present in the native state. An 8 kDa band from P11C<sub>1-135</sub> was weaker than in the P11C<sub>1-135</sub>-Ca<sup>2+</sup>-pdTp complex suggesting a local heterogeneity or higher mobility for this region of the fragment. In addition, a 7 kDa band from the cleavage of K64C<sub>1-135</sub> is weaker in the K64C<sub>1-135</sub>-Ca<sup>2+</sup>-pdTp complex and similar to the band obtained in the presence of 4.8 M urea. This again suggests local disorder.

Several specific cleavage products of the SNase<sub>1-135</sub> variants generated in the absence of ligands were isolated and characterized (Table 1). The cleavage sites found previously for the full length versions of these mutants are also included for comparison<sup>23</sup>. The sites of EDTA-Fe attachment and cleavage are shown in Fig. 4 and 5. The N-terminal region of the native protein forms an antiparallel  $\beta$ -meander composed of strands 1-3; the P11C substitution is within the first  $\beta$ -strand. Cleavage of nuclease P11C occurs at position 28 within the  $\beta$ -turn connecting strand 2 and 3. Since the cleavage yield at position 28 is similar with and without ligands (figure 3, lanes 2 and 3), we conclude that the  $\beta$ -meander is stably formed in the SNase 1-135 fragment.

The  $\beta$ -meander forms a five-stranded  $\beta$ -barrel by interacting with a  $\beta$ -hairpin formed by strand 4 and 5. The 8 kDa product observed in the SDS-PAGE (Fig. 3a) represents cleavage at residues 71-72 in  $\beta$ -strand 4 as observed for full length nuclease (Table 1). Thus, it is likely that the  $\beta$ -barrel has a native-like topology. Since the yield of this cleavage product is lower than in the folded state, the  $\beta$ -barrel may be expanded and

loosely packed. Additional cleavage products mapped to residues 96 and 99 in the loop connecting helix 2 with the  $\beta$ -barrel. These are minor cleavage products since their expected N-terminal parts are seen as a faint band of about 10 kDa in the SDS-PAGE analysis. A comparable band was observed in the cleavage of full-length SNase P11C but could not be isolated and characterized<sup>23</sup>. These cleavage sites report the native interaction between helix 2 and the  $\beta$ -structure.

K64C-EDTA-Fe and its corresponding truncated version K64C<sub>1-135</sub>-EDTA-Fe were both cleaved at residue 102. This particular cleavage product maps the native interaction between helix 1 and 2 of nuclease<sup>23</sup>. Also, cleavage sites observed in  $\beta$ -strand 4 and at the end of helix 2 closely matched cleavage observed in full length nuclease (Table 1). These results agreed with those obtained with the P11C variant and confirmed that, in the partially folded state, the polypeptide backbone spanning the  $\beta$ -barrel-helix-1-helix 2 system is following a native-like topology. Additional cleavage sites found for K64C<sub>1-135</sub> at residues 108-112 indicated that helix 3 is not packing against the remainder of the molecule. These sites, found in the connecting segment between helix 2 and 3 are not accessible in the folded structure, but would be exposed if the molecule is expanded displacing helix 3 from helix 2 and the  $\beta$ -sheet structure, and if the conformation of the connecting loop is segmentally disordered (figure 4b).

The proposed disorder of helix 3 and its connecting loop to helix 2 was probed with the SNase<sub>1-135</sub> H124C variant. The attachment site occurs on helix 3 and cleavage of full length H124C-EDTA in the native state occurs at Ala 102 in helix 2. Residues 102 and 124 are located in two adjacent helices (H2 and H3 respectively) separated by 11.34 Å (distance C $\alpha$ <sub>102</sub>-C $\alpha$ <sub>124</sub>) in the native fold of the protein (Fig. 5). As pointed out before, the K64C (in helix 1) variant also yields cleavage at Ala 102 (in helix 2). Both results are consistent with the proximity of helix 1, 2, and 3, which run parallel and pack against each other in the native structure of the protein. The H124C site follows a type VI<sub>a</sub>  $\beta$ -turn (residues 115-118) containing a *cis* K116-P117 peptide bond that is in

equilibrium with the *trans* configuration<sup>29-32</sup> This region is under strain and is thus a good candidate for local unfolding prior to the global unfolding transition<sup>33</sup>. As shown in Fig. 3, the band from cleavage at position 102 is absent in the case of truncated H124C<sub>1-135</sub>-EDTA-Fe without ligands or in 4.8 M urea. The addition of Ca<sup>2+</sup> and pdTp restores this cleavage site as proven by sequencing of the PVDF blotted fragments. Thus, stabilization of the SNase 1-135 fragment into a native-like state, by ligands, seems to proceed through the incorporation of helix 3 to the already formed native-like core.

The local cleavage around residue 124 for full-length nuclease reflects the geometry and solvent exposure of the C-terminal  $\alpha$ -helix<sup>23</sup>, with cleavage sites separated by 3-4 residues, extending through residue 131 in the exposed face of the helix. Only cleavage at site 127 was detected in this region of the ligand stabilized SNase 1-135 H124C fragment. This may be due to the low yield of these products or to alteration of the local geometry even in the presence of ligands.

#### **Cleavage mapping results indicate that the backbone fold of the SNase fragments is mostly native-like**

The cleavage results for all the nuclease variants analyzed with this technique lead us to propose the structure illustrated in Fig. 4 for the nonnative state of staphylococcal nuclease. In this model, most of the conformation is native-like with the exception of the segment comprising helix 3 and the connecting loop between helix 2 and 3. The chemical cleavage pattern described for the nuclease fragments shares similarities with that found for the related full length nuclease variants. This indicates a common proximity of sites and common solvent accessibility in the native and nonnative states. Novel cleavage sites are observed at residues that would be buried in the native structure but become exposed by the unfolding of helix 3. Taken together, these data are consistent with a surprisingly native-like conformation for much of SNase<sub>1-135</sub>.

## Comparison with NMR analysis of related SNase fragments

The optical and hydrodynamic properties of the SNase<sub>1-135</sub> fragments examined herein are similar to the SNase<sub>1-136</sub> fragment studied earlier. Unfortunately, the NMR analysis of the SNase<sub>1-136</sub> fragment proved intractable due to very poor dispersion of the NMR signals<sup>34</sup>. A single amino acid substitution in the SNase<sub>1-136</sub> sequence, G88V, (an *m*- variant), shifted the conformational ensemble toward the native state facilitating structural analysis by NMR spectroscopy. SNase<sub>1-136</sub> G88V showed a decreased  $R_g$ <sup>28</sup>, increased  $\alpha$ -helix content and increased NMR chemical shift dispersion compared to SNase<sub>1-136</sub> and the fragments studied in this work. Application of 2D and 3D NMR methods to <sup>15</sup>N and <sup>13</sup>C labeled SNase<sub>1-136</sub> G88V allowed assignment of most backbone atoms, however few side chains could be assigned and no side chain-side chain NOE's were identified. Backbone-backbone NOE's were used to identify a native-like structure in the  $\beta$ -barrel region and  $NH_i-NH_{i+1}$  NOE's were used to identify the presence of native-like  $\alpha$ -helical regions. However, no NOE's were observed to experimentally position the  $\alpha$ -helical segments with respect to each other or the  $\beta$ -barrel<sup>34</sup>.

Interestingly, the number of long range NOE's used to define the structure of the SNase 1-136 G88V fragment was comparable to the number of cleavage sites used in developing the model presented herein for the less structured SNase 1-135 fragment. Further, the larger range of distances mapped by the chemical cleavage technique allows us to define the proximity of secondary structure elements, particularly  $\alpha$ -helix 1 and 2 that could not be placed in the structure of SNase 1-136 G88V by NMR data alone. The chemical cleavage analysis provided structural information concerning the nonnative SNase state that was in agreement with, and complementary to, NMR data derived from a more structured nonnative state of the protein. Thus, the chemical cleavage technique can identify native-like structures in situations where NMR analysis is extremely difficult or not possible.

More recently a fragment of the native protein, with an N- and C-terminal deletion, SNase  $\Delta$ 131 $\Delta$  has been investigated by NMR spectroscopy. Multi-dimensional triple resonance NMR of SNase  $\Delta$ 131 $\Delta$  enriched with  $^{13}\text{C}$  and  $^{15}\text{N}$  allowed the sequence-specific assignment for 106 of the 131 residues<sup>35</sup>.  $\alpha$ -helix segments were identified which correspond to two of the three  $\alpha$ -helices in the native state. The C-terminal segment that is the third  $\alpha$ -helix in the native state showed no evidence of regular structure in SNase  $\Delta$ 131 $\Delta$ . Dynamic considerations suggest that the persistent  $\alpha$ -helix structure is in rapid equilibrium with a disordered conformation. Except for a weak NOE between the NH protons of E52 and E43 no other NOE from long-range tertiary interactions could be assigned, even though at least ten cross-peak in the  $3\text{D}^1\text{H}\{^{15}\text{N}\}$ NOESY-HMQC spectrum arise from non sequential interactions. This work dramatizes the difficulties of an NMR structural analysis of nonnative states despite valiant efforts to apply state of the art NMR methods.

## Conclusions

The theoretical model of Ptitsyn for the molten globule<sup>3</sup>, with nonuniform expansion and local disorder but with residues occupying approximately native positions, appears to properly describe the nonnative state of SNase<sub>1-135</sub>. The chemical cleavage analysis of SNase<sub>1-135</sub> fragment complements the previous NMR analysis and extends our understanding of the structure of this nonnative state. The manner in which the partial native-like structure of this and other nonnative proteins states are stabilized without the apparent presence of specific tertiary interactions is now a major problem in the field of protein folding. The chemical cleavage method should provide a useful structural tool for the analysis of these nonnative states.

## Methods

### Production of nuclease variants.

Truncated staphylococcal nuclease variants were produced by PCR site-directed mutagenesis of the wild-type nuclease gene cloned into M13jg18<sup>36</sup>. The construct was cloned into pAS1 under the control of  $\lambda$ P<sub>L</sub> promoter and transformed into *E. coli* strain AR120. After induction, cells were lysed with 8 M urea; and subsequently, over expressed nuclease variants were purified and analyzed as described previously<sup>21</sup>.

#### **Preparation of EPD-Fe-modified proteins.**

Protein-EDTA-Fe conjugates were prepared as described <sup>23</sup>. Briefly, P11C<sub>1</sub>-135, T13C<sub>1</sub>-135, K70C<sub>1</sub>-135, and H124C<sub>1</sub>-135 nuclease variants were dissolved in 100 mM HEPES, pH 7.0 and immediately reacted with EPD-Fe (0.75 mM protein and 1.5 mM EPD-Fe in 100  $\mu$ l total volume). The solution was incubated at room temperature for 1 h. The protein-EDTA-Fe conjugate was then purified from residual EPD-Fe and thiopyridone by spin-column chromatography<sup>37</sup> using Bio-Gel P2 (100-200 Mesh, Bio-Rad) equilibrated in 75 mM reaction buffer. The coupling reaction was complete as shown by titration of the residual free thiol group with DTNB<sup>38</sup>. The cleavage reaction was carried out for 30 min at 23 °C in 50 mM HEPES, pH 7.0, with a protein concentration of 15  $\mu$ M.

#### **The cleavage reaction and product analysis.**

The reaction was initiated by adding ascorbate pH 7.0 to give a final concentration of 20 mM. Unless otherwise indicated, the reaction was terminated by adding 2-mercaptoethanol to give 4% (v/v) final solutions. Samples for SDS-PAGE analysis were frozen (-70 °C), freeze -dried, dissolved in SDS-PAGE sample buffer, heated 10 min at 56 °C, and electrophoresed. Molecular weight markers used in this and previous works<sup>21,23</sup> were from the same kit of myoglobin fragments provided by Pharmacia-LKB. However, molecular weight assignment has been changed herein because the company technical information proved to be partly incorrect<sup>39</sup>. The new assignment does not affect the conclusions drawn in our previous papers. SDS-PAGE

and blotting onto PVDF membranes<sup>40</sup> was used to isolate the fragmentation products submitted to N-terminal sequencing. Reverse phase HPLC analysis of the fragmentation products was performed after a size exclusion chromatography step as described<sup>23</sup>.

#### **Size exclusion chromatography of nuclease variants.**

$R_S$  was determined as described by Uverski<sup>41</sup> at room temperature using a calibrated Superose 6 column (Pharmacia) attached to a HPLC system (RAINING) with detection at 215 nm. The solvent was 50 mM HEPES, 200 mM NaCl, pH 7.0. A range of protein concentration was tested to assess the aggregation state and compactness of the fragments under the conditions for the cleavage reaction (0.2 mg/ml).  $R_S$  was extrapolate to zero protein concentration

#### **Circular dichroism spectroscopy.**

CD spectra were obtained using an Aviv Circular Dichroism DS-62 spectropolarimeter at 25 °C in either 2.5 mM HEPES, 50 mM NaCl, pH 7.0, or 2.5 mM HEPES, 50 mM NaCl, 10 mM CaCl<sub>2</sub>, 1mM pdTp, pH 7.0. The cuvette path length was 0.1 cm and the protein concentration was between 5-15  $\mu$ M (determined by amino acid analysis of four aliquots of each fragment solution). Data were collected every 0.5 nm at 1 s interval with a 1.5 nm bandwidth. Seven scans were averaged for each sample and the average spectra were smoothed using a fourth-order polynomial function and a ten point window after buffer subtraction.

FIG. 1 a, Structure of EDTA-Fe covalently linked to a cysteine residue through a disulfide bridge. A disulfide exchange reaction between a protein containing a free accessible thiol group and EPD-Fe<sup>21</sup> leads to the covalent attachment of the hydrophilic EDTA-Fe moiety to the polypeptide backbone. The attachment reaction is quantitative and specific for thiol groups. b, Reaction of the protein -EDTA-Fe conjugated with ascorbate and oxygen produces reactive oxygen species which, in turn, cause the conformation-dependent cleavage of the polypeptide backbone<sup>21</sup>. The fully unfolded state is represented by a straight line to highly the absence of specific interactions between different segments of the chain. A folded state is represented as a meander to illustrated any persistent and specific fold of the chain. The cloud in each structure represents the allowed iron positions in space without steric clashes with protein atoms. The analysis of the cleavage products by SDS-PAGE, Edman degradation or mass spectrometry allows the tertiary fold of the chain in the vicinity of the cysteine bearing the chelator to be inferred<sup>23</sup>.

FIG. 2 a, stokes radii of nuclease variants determined by size exclusion chromatography. ▽, wild type nuclease; ◇, P11C; ◆, P11C-EDTA-Fe; ○, P11C<sub>1-135</sub>; ●, P11C<sub>1-135</sub>-EDTA-Fe; □, K64C<sub>1-135</sub>; ■, K64C<sub>1-135</sub>-EDTA-Fe; △, H124C<sub>1-135</sub>; ▲, H124C<sub>1-135</sub>-EDTA-Fe. The arrows indicate the Stockes radii of wild-type nuclease and the K64C<sub>1-135</sub> fragment in the presence of 1.5 M GuHCl. At the protein concentration used for the cleavage experiments, all nuclease variants are monomeric. Only one of the mutants, P11C<sub>1-135</sub> shows a tendency to associate at higher protein concentrations. The expected  $R_g$ s based upon calibration curves and standard proteins in gel filtration experiments<sup>41</sup> for full-length nuclease as monomer, dimer and in the completely unfolded state are 20.2, 26.1 and 37.9 Å respectively. Small-angle scattering measurements gave an estimate of 33.0 Å for the  $R_g$  of SNase in 8M urea<sup>28</sup>. Based on theoretical considerations, the  $R_g$  of a fully unfolded polypeptide of this size should be

larger than 40 Å<sup>42</sup>. The difference has been ascribed to nuclease persistent residual structure under denaturing conditions<sup>28</sup>. b, circular dichroism analysis of EPD-Fe modified truncated nuclease variants. Analysis was performed at 25 °C in 2.5 mM HEPES, 50 mM NaCl, pH 7.0, either with or without 10 mM CaCl<sub>2</sub> and 1mM pdTp (to induce folding). (—), P11C<sub>1-135</sub>EDTA-Fe; (-----), K64C<sub>1-135</sub>-EDTA-Fe; and (.....), H124C<sub>1-135</sub>-EDTA-Fe. The liganded complexes are superposed with deeper troughs at 208 and 222 nm. a, Size exclusion chromatography of nuclease variants. ∇, wild type nuclease; ◇, P11C; ◆, P11C-EDTA-Fe; O, P11C<sub>1-135</sub>; ●, P11C<sub>1-135</sub>-EDTA-Fe; □, K64C<sub>1-135</sub>; ■, K64C<sub>1-135</sub>-EDTA-Fe; Δ, H124C<sub>1-135</sub>; ▲, H124C<sub>1-135</sub>-EDTA-Fe.

FIG. 3 SDS-PAGE analysis of the cleavage products. Panels A, B, and C correspond to P11C<sub>1-135</sub>-EDTA-Fe, K64C<sub>1-135</sub>-EDTA-Fe, and H124C<sub>1-135</sub>-EDTA-Fe respectively. Lane 1: Blank, the reaction was stopped at time zero by adding 4% 2-mercaptoethanol before ascorbate. Lane 2: Standard cleavage reaction (see Methods). Lane 3: Cleavage reaction after a 30 min incubation with 10 mM CaCl<sub>2</sub> and 1 mM pdTp (nuclease ligands). Lane 4: Cleavage reaction in the presence of 4.8 M urea. Under standard reaction conditions the P11C and K64C fragments have cleavage patterns remarkably similar to their previously studied full length counterparts whereas a completely different pattern is seen for the H124C fragment. Upon addition of Ca<sup>2+</sup> and pdTp, the cleavage patterns in panels A and B do not change; however, in panel C a new pattern is produced that is strikingly similar to that of the full length mutant. This suggests that under standard reaction conditions, helix 3 of the fragment is in an environment that differs substantially from that experienced in the folded full length protein. Incubation with calcium and pdTp results in restoration of the native cleavage pattern.

FIG. 4 Proposed model for SNase<sub>1-135</sub> based on the cleavage mapping results showing the sites of reagent attachment (cyan) as well as the sites of cleavage (red) detected for

each of the truncated fragments. The model was built using wild type SNase coordinates<sup>43</sup> for residues 1-104. Residues 105 through 135 were modeled in a partly extended conformation using X-PLOR<sup>44</sup>. Cleavage sites for K64C mapping this segment were constrained to within 15 Å of the site of reagent attachment. A, P11C<sub>1-135</sub>-EDTA-Fe; B, K64C<sub>1-135</sub>-EDTA-Fe

FIG 5 Ribbon trace of SNase truncated at residue 135 showing the relative positions of EDTA-Fe attached to residue 124 (cyan) and the cleavage sites (red) detected for H124CEDTA-Fe 1-135 in the presence of Ca<sup>2+</sup> and pdTp. These ligands drive the partly folded state of SNase fragments toward a native-like state.

---

TABLE 1 Cleavage sites of full length and truncated staphylococcal nuclease.

---

Protein	Cleavage sites <sup>a</sup>
P11C <sub>1-135</sub>	<b>28</b> , <b>71-72<sup>b</sup></b> , 99, 96
P11C	15, <b>28</b> , 29, 64, <b>71</b> , <b>72</b>
K64C <sub>1-135</sub>	70, 72, 74, 99, <b>102</b> , 106, 108, 110, 111, 112
K64C	60, 71, 97, <b>102</b> , 105
H124C <sub>1-135</sub> <sup>c</sup>	<b>102</b> , 103, <b>127</b>
H124C	<b>102</b> , 121, 122, <b>127</b> , 131

<sup>a</sup>Sites were aligned in bold to highlight similarities in cleavage pattern.

<sup>b</sup>All reported cleavage sites were determined by Edman degradation of the isolated C-terminal reaction product. The only exception was cleavage at sites 71-72 that was inferred from the product mobility in SDS-PAGE analysis and the sequencing of the corresponding N-terminal cleavage fragment. <sup>c</sup>Cleavage of H124C<sub>1-135</sub> was performed in the presence of Ca<sup>2+</sup> and pdTp.

ACKNOWLEDGMENTS: This work was supported by the Howard Hughes Medical Institute and a Fogarty International Research Collaboration Award from the NIH. D.W.L. is a Department of Defense Air Force Laboratory Graduate Fellow. We thank the W.M. Keck Foundation Biotechnology Resource Laboratory at the Yale University School of Medicine and The Laboratorio Nacional de Investigación y Servicios-Proteínas for amino acid analysis and peptide sequencing. We thank Fred Richards for helpful discussions, Paul Harkins for the molecular dynamic simulation, Isobel Parsons, Alan Robertson, and Alex Golden for technical assistance.

---

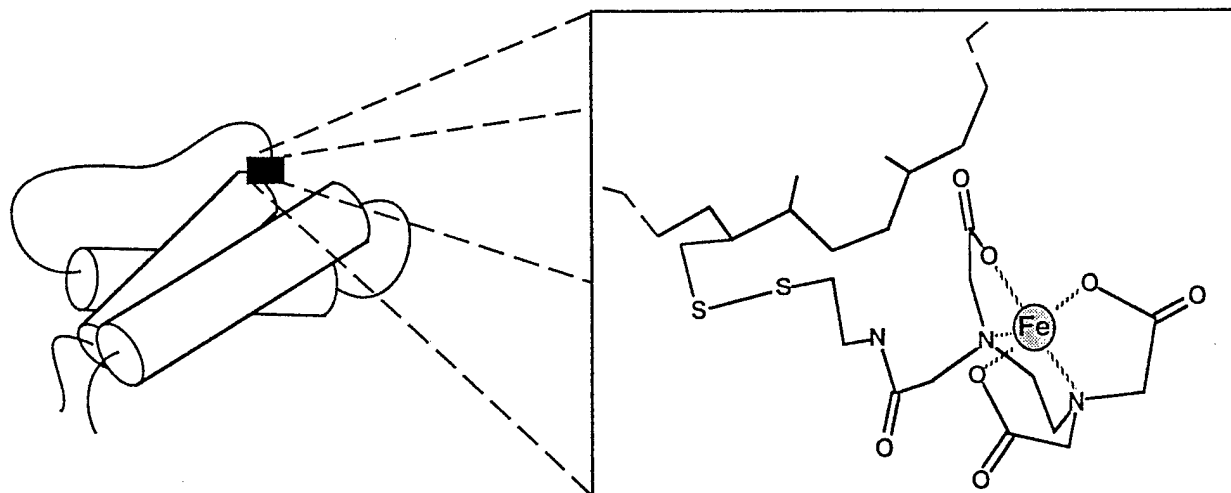
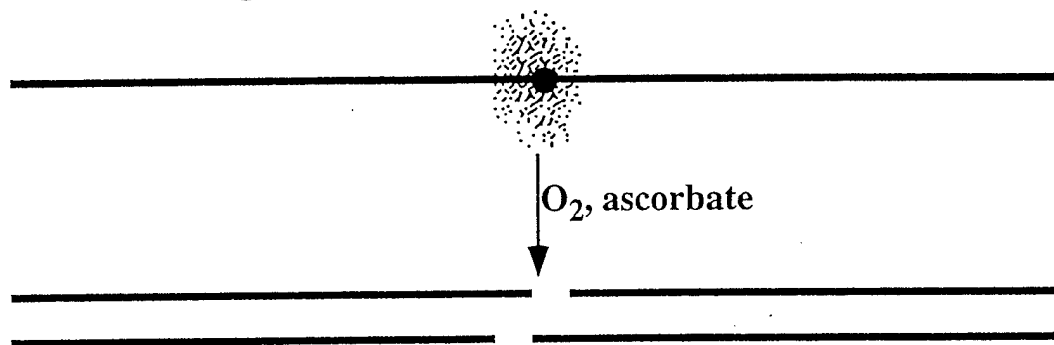
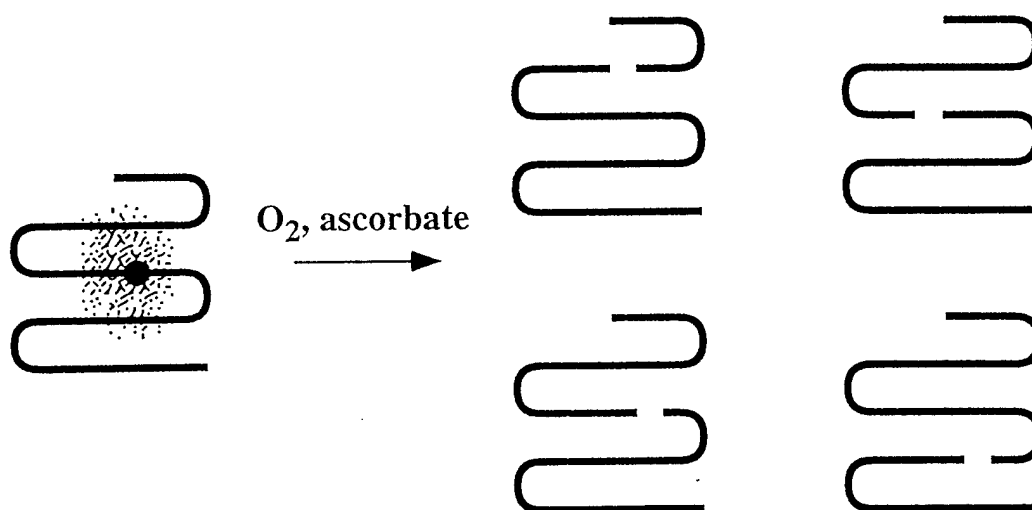
1. Kim, P. S. & Baldwin, R. L. Intermediates in the folding reaction of small proteins. *Annu. Rev. Biochem.* **59** 631-660 (1990).
2. Matthews, C. R. Pathways of protein folding *Annu. Rev. Biochem.* **62** 653-683 (1993).
3. Ptitsyn, O. B. in *Protein Folding* (ed. Creighton, T. E.) 243-300 (New York, W. H. Freeman and Company, 1992).
4. Buck, M., Radford, S. E. & Dobson, C. M. Amide hydrogen exchange in a highly denatured state. *J. molec. Biol.* **237** 247-254 (1994).
5. Baum, J., Dobson, C. M., Evans, P. A. & Hanley, C. Characterization of a partly folded protein by NMR methods: studies on the molten globule state of guinea pig  $\alpha$ -lactalbumin. *Biochemistry* **28** 7-13 (1989).
6. Radford, S. E., Buck, M., Topping, K. D., Dobson, C. M. & Evans, P. A. Hydrogen exchange in native and denatured states of hen egg-white lysozyme. *Proteins* **14** 237-248 (1992).
7. Hughson, F. M., Wright, P. E. & Baldwin, R. L. Structural characterization of a partly folded apomyoglobin intermediate. *Science* **249** 1544-1548 (1990).
8. Chyan, C. L., Wormald, C., Dobson, C. M., Evans, P. A. & Baum, J. Structure and stability of a molten globule state of guinea pig  $\alpha$ -lactalbumin: a hydrogen exchange study. *Biochemistry* **32** 5681-5691 (1993).

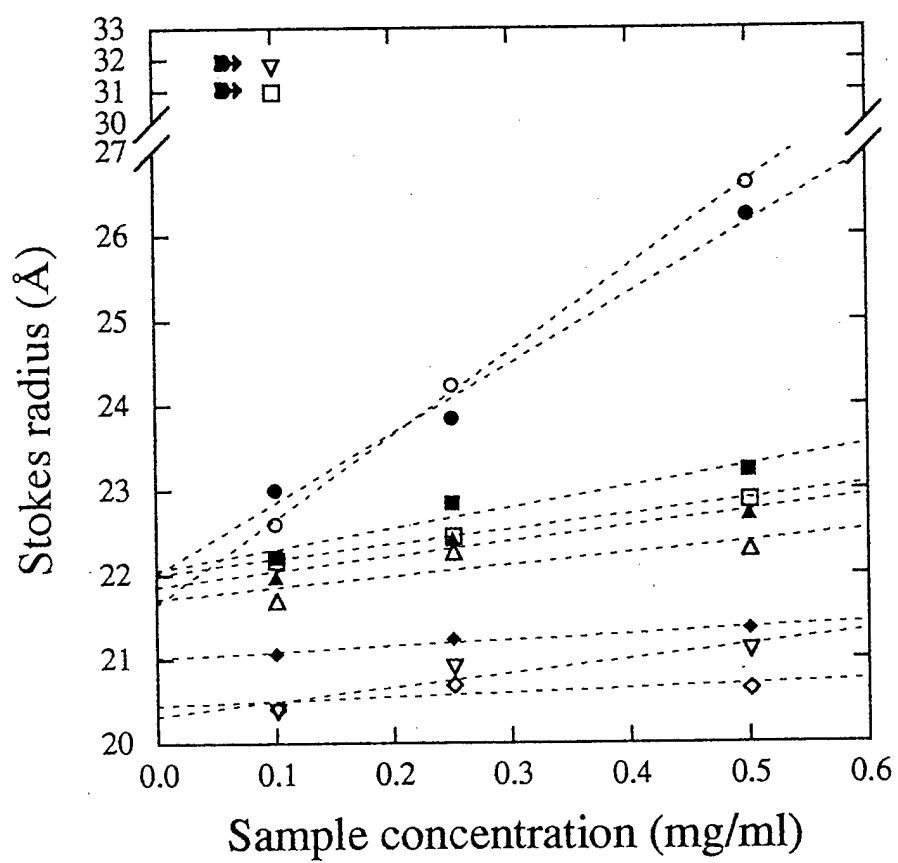
- 
9. Koide, S., Dyson, H. J. & Wright, P. E. Characterization of a folding intermediate of apoplastocyanin trapped by proline isomerization. *Biochemistry* **32** 12299-12310 (1993).
  10. Englander, S. W. & Mayne, L. Protein folding studied using hydrogen-exchange labeling and two-dimensional NMR. *Annu. Rev. Biophys. Biomol. Struct.* **21** 243-265 (1992).
  11. Baldwin, R. L. Pulsed H/D-exchange studies of folding intermediates. *Current Opinion in Structural Biology* **3** 84-91 (1993).
  12. Jeng, M. F., Englander, S. W., Elove, G. A., Wand, A. J. & Roder, H. Structural description of acid denatured cytochrome c by hydrogen exchange and 2D NMR. *Biochemistry* **29** 10433-10437 (1990).
  13. Alexandrescu, A. T., Evans, P. A., Pitkeathly, M., Baum, J. & Dobson, C. M. Structure and dynamic of the molten globule state of guinea pig  $\alpha$ -lactalbumin: a two-dimensional NMR study. *Biochemistry* **32** 1707-1718 (1993).
  14. Jennings, P. A. & Wright, P. E. Formation of a molten globule intermediate early in the kinetic folding pathway of apomyoglobin *Science* **262** 892-896.
  15. Ptitsyn, O. B., Semisotnov, G. V. in Conformations and forces in protein folding (ed Nall, B. T. & Dill, K. A.) 155-168 (American Association for the Advancement of Science, Washington, D. C. 1991).
  16. Karplus, M. & Shakhnovich, E. in Protein Folding (ed. Creighton, T. E.) 127-195 (New York, W. H. Freeman and Company, 1992).
  17. Peng, Z. Y & Kim, P. S. A protein dissection study of a molten globule. *Biochemistry* **33** 2136-2141 (1994).
  18. Lattman, E. E., Fiebig, K. M. & Dill, K. A. Modeling compact denatured states of proteins. *Biochemistry* **33** 6158-6166 (1994)

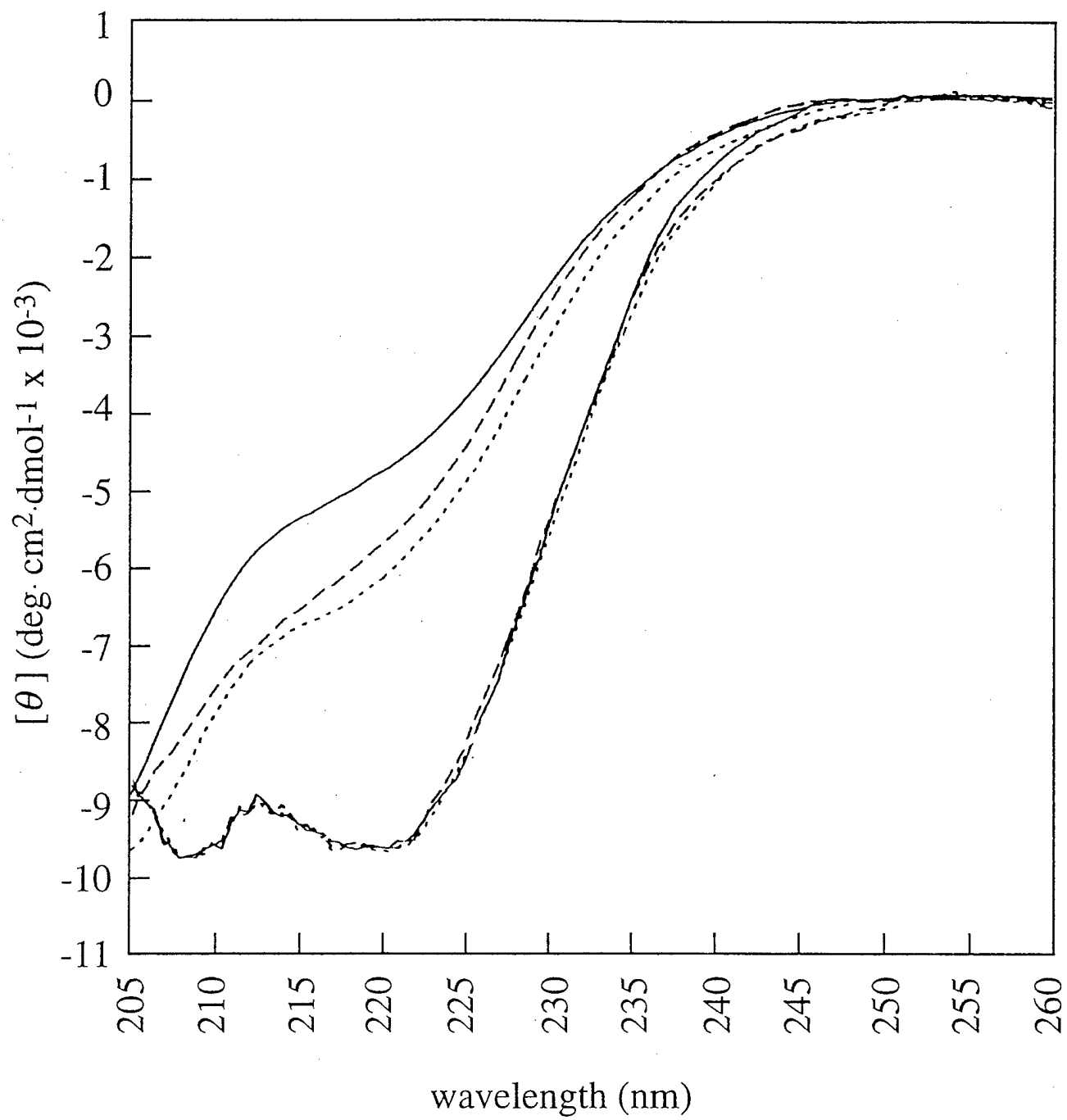
- 
19. Wagner, G., Hyberts, S. G. & Havel, T. F. NMR structure determination in solution: a critique and comparison with x-ray crystallography. *Annu. Rev. Biophys. Biomol. Struct.* **21** 167-198 (1992).
  20. Dobson, C. M., Hanley, C., Radford, S. E., Baum, J., & Evans, P. A. in Conformations and forces in protein folding ( ed Nall, B. T. & Dill, K. A.) 175-181 (American Association for the Advancement of *Science*, Washington, D. C. 1991).
  21. Ermácora, M. R., Delfino, J. M.; Cuenoud, B., Schepartz, A & Fox, R. O. Conformation-dependent cleavage of staphylococcal nuclease with a disulfide-linked iron chelate. *Proc. natl. Acad. Sci.* **89** 6383-6387 (1992).
  22. Platis, I. E., Ermácora, M. R. & Fox, R. O. Oxidative polypeptide cleavage mediated by EDTA-Fe covalently linked to cysteine residues. *Biochemistry* **32** 12761-12767 (1993).
  23. Ermácora, M. R., Ledman D. W., Hellings, H. W., Hsu, G. W. & Fox R. O. Mapping staphylococcal nuclease conformation using an EDTA-Fe derivative attached to genetically engineered cysteine residues. *Biochemistry* **33** 13625-13641 (1994).
  24. Shortle, D. & Meeker, A. K. Mutant forms of staphylococcal nuclease with altered patterns of guanidine hydrochloride and urea denaturation. *Proteins* **1**, 81-89 (1986).
  25. Carra, J. H. & Privalov, P. L. Energetics of denaturation and m values of staphylococcal nuclease mutants. *Biochemistry* **34** 2034-2041 (1995).
  26. Shortle, D. & Meeker, A. K. Residual structure in large fragments of staphylococcal nuclease: effects of amino acid substitutions. *Biochemistry* **28** 936-944 (1989)
  27. Flanagan, J. M., Kataoka, M., Shortle, D. & Engelman, D. M. Truncated staphylococcal nuclease is compact but disordered. *Proc. natl. Acad. Sci.* **89** 748-752 (1992).

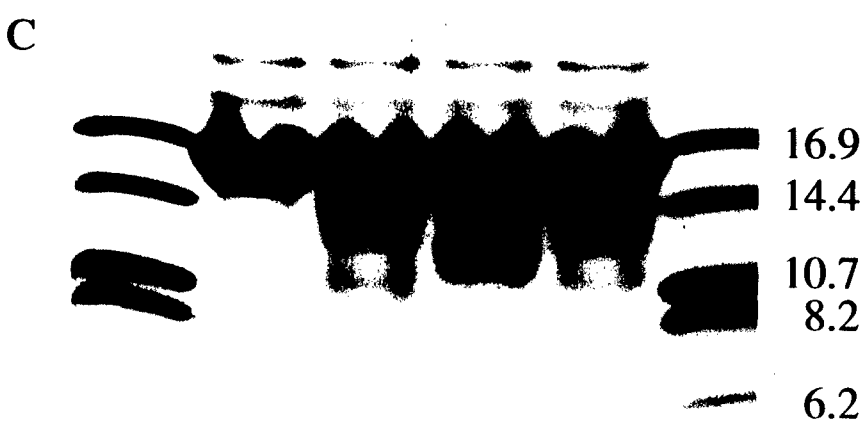
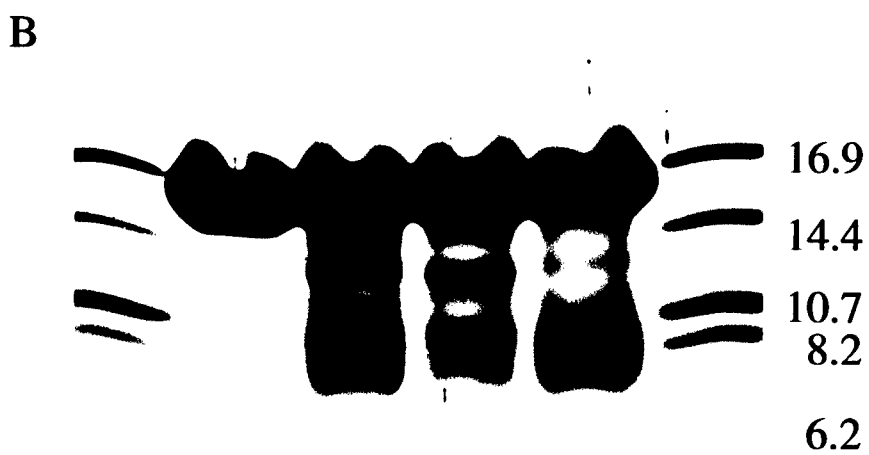
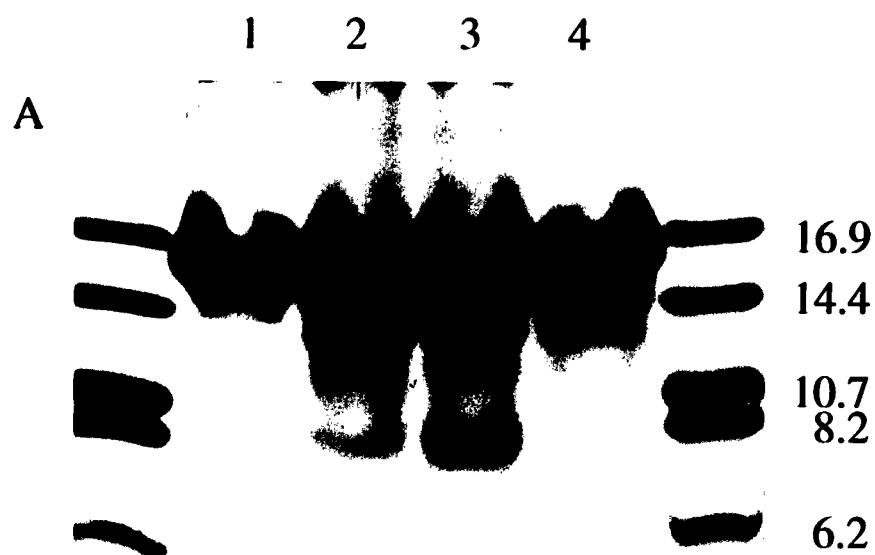
- 
28. Flanagan, J. M., Kataoka, M., Fujisawa, T. & Engelman, D. M. Mutations can cause large changes in the conformation of a denatured protein *Biochemistry* **32** 10359-10370 (1993).
29. Nakano, T., Antonino, L. C., Fox, R. O. & Fink, A. L. Effect of proline mutation on the stability and kinetics of folding of staphylococcal nuclease. *Biochemistry* **32** 2534-2541 (1993).
30. Chen, H. M., Markin, V. S., & Tsong, T. Y pH induced folding/unfolding of staphylococcal nuclease: determination of kinetic parameters by the sequential-jump method. *Biochemistry* **31** 1483-1491 (1992).
31. Evans, P. A., Kautz, R. A., Fox, R. O. & Dobson, C. M. A magnetic transfer resonance study of the folding of staphylococcal nuclease. *Biochemistry* **28** 362-370 (1989).
32. Alexandrescu, A. T., Ulrich, E. L. & Markley, J. L. Hydrogen-1 NMR evidence for three interconverting forms of staphylococcal nuclease: effects of mutations and solution conditions on their distribution. *Biochemistry* **28** 204-211 (1989).
33. Hodel, A., Kautz, R. A., Jacobs, M. D., & Fox, R. O. Stress and strain in staphylococcal nuclease. *Prot. Sci.* **2** 838-850 (1993).
34. Shortle, D., & Abeygunawardana, C. NMR analysis of the residual structure in the denatured state of an unusual mutant of staphylococcal nuclease *Structure* **1** 121-134 (1993).
35. Alexandrescu, A.T., Abeygunawardana, C., & Shortle, D. Structure and dynamic of a denatured 131-residue fragment of staphylococcal nuclease: a heteronuclear study. *Biochemistry*, **33** 1063-1072 (1994).
36. Hynes, T. R., Kautz, R. A., Goodman, M. A., Gill, J. F. & Fox, R. O. Transfer of a  $\beta$ -turn structure to a new protein context. *Nature* **339** 73-76 (1989).

- 
37. Penefsky, H. S. A centrifuged-column procedure for the measurement of ligand binding by beef heart F<sub>1</sub>. *Meths Enzymol.* **56** 527-530 (1979).
  38. Ellman, G. L. Tissue sulfhydryl groups *Arch. Biochem. Biophys.* **82** 70-77 (1959).
  39. Kratzin, H. D., Wiltfang, J., Karas, M., Neuhoff, V. & Hilschmann, N. Gas-phase sequencing after electroblotting on polyvinylidene difluoride membranes assigns correct molecular weights to myoglobin molecular weight markers. *Anal. Biochem.* **183** 1-8 (1989).
  40. Matsudaira, P. Sequence from picomole quantities of proteins electroblotted onto polyvinylidene difluoride membranes. *J. biol. Chem.* **262** 10035-10038 (1987).
  41. Uversky, V. N. Use of fast protein size-exclusion liquid chromatography to study the unfolding of proteins which denature through the molten globule. *Biochemistry* **32** 13288-13298 (1993).
  42. Miller, W. G. & Goebel, C. V. Dimensions of protein random coils. *Biochemistry* **7** 3925-3935 (1968).
  43. Hynes, T. R. & Fox, R. O. The crystal structure of staphylococcal nuclease refined at 1.7 Å resolution. *Proteins* **10** 92-105 (1991)
  44. Brünger, A. T. A system for X-ray crystallography and NMR (Yale Univ. Press, New Haven, CT, 1992)

**a****Protein-EDTA-Fe conjugate****b****Cleavage reaction in the fully unfolded state****Cleavage reaction in a folded state**









\_\_\_\_\_



# Biochemistry®

---

## **Mapping Staphylococcal Nuclease Conformation Using an EDTA–Fe Derivative Attached to Genetically Engineered Cysteine Residues**

---

***Mario R. Ermácora, David W. Ledman,  
Homme W. Hellinga, Gene W. Hsu, and Robert O. Fox***

---

*The Howard Hughes Medical Institute and The Department of  
Molecular Biophysics and Biochemistry, Yale University,  
266 Whitney Avenue, New Haven, Connecticut 06520*

Reprinted from  
BIOCHEMISTRY, Volume 33, Number 48, Pages 13625–13641

Copyright © 1994 by the American Chemical Society  
and reprinted by permission of the copyright owner

# Mapping Staphylococcal Nuclease Conformation Using an EDTA–Fe Derivative Attached to Genetically Engineered Cysteine Residues<sup>†</sup>

Mario R. Ermácóra,<sup>‡,§,||</sup> David W. Ledman,<sup>§</sup> Homme W. Hellinga,<sup>§,⊥</sup> Gene W. Hsu,<sup>§,¶</sup> and Robert O. Fox<sup>\*,‡,§</sup>

The Howard Hughes Medical Institute and The Department of Molecular Biophysics and Biochemistry, Yale University, 266 Whitney Avenue, New Haven, Connecticut 06520

Received March 23, 1994; Revised Manuscript Received July 15, 1994<sup>®</sup>

**ABSTRACT:** Six single cysteine variants of staphylococcal nuclease were reacted with the iron complex of (EDTA-2-aminoethyl) 2-pyridyl disulfide (EPD–Fe) [Ermácóra, M. R., Delfino, J. M., Cuenoud, B., Schepartz, A., & Fox, R. O. (1992) *Proc. Natl. Acad. Sci. U.S.A.* 89, 6383–6387] and used to assess the ability of this cleavage reagent to faithfully report on the structure of nonnative protein states. The act of mutation and modification did not significantly alter the protein's global structure, as measured by CD and enzymatic activity, and only modestly affected its stability. The reaction was conformation dependent and generated specific cleavage products that mapped tertiary interactions present in the folded state. Several parameters relevant to the cleavage reaction and its use as a conformational probe were analyzed. Proximity and solvent accessibility are the most important parameters in determining the cleavage pattern and can be used to predict cleavage sites in the native protein. The cleavage reaction can be performed in the presence of high denaturant concentration, in the presence of SDS, and under a wide range of pH values; thus it can readily be applied to the study of equilibrium folding intermediates. Mass spectrometric analysis combined with N-terminal sequencing identified cleavage products consistent with a single cleavage event per protein molecule and revealed one cleavage mechanism which was not previously considered for protein oxidative degradation, although it was reported for hydroxyl radical induced cleavage of small peptides. Identification of the cleavage sites obtained from each variant allowed a nearest-neighbor mapping of the secondary structural elements of nuclease. Quantitation of specific cleavage products was used to monitor the disruption of the interaction between helices H2 and H3 in equilibrium unfolding experiments. The resulting unfolding curve revealed a local conformational heterogeneity at low denaturant concentration which was not observed when the same transition was monitored by the change in fluorescence of a single nuclease tryptophan. Interestingly, the midpoint of the transition and the second half of the unfolding curve were the same, as monitored by the two probes. This indicates that the lifetime of the reactive oxygen species generated by the cleavage reagent is short compared to the unfolding equilibrium rate constants and that the cleavage technique identifies a native-like folding intermediate not detected by fluorescence. The experiments presented herein demonstrate that EPD–Fe-mediated protein cleavage is an appropriate technique for the study of nonnative protein structure. The method should be most powerful as a difference technique for comparing native and nonnative protein states, especially when combined with NMR data.

Nonnative states of proteins, including the molten globule, can be populated at equilibrium and are thought to represent conformations adopted along the protein folding pathway (Jennings & Wright, 1993). Optical spectroscopies and low-angle X-ray scattering have been used to examine the global properties of these states (Goto et al., 1990; Flanagan et al., 1992; Mach et al., 1993; Matthews et al., 1993). NMR

spectroscopy can sometimes be used to identify specific close contacts within protein nonnative states through NOE measurements; however, technical difficulties can limit the usefulness of this technique.

Recently, we proposed the use of a chemical cleavage technique that could complement NMR spectroscopy in the investigation of nonnative protein structures by identifying regions of the protein backbone that are adjacent to each other (Ermácóra et al., 1992). The approach involves the covalent attachment of EPD–Fe<sup>1</sup> (an EDTA–Fe analog) to a single genetically engineered cysteine site on a protein surface, followed by reduction of the iron with ascorbate.

<sup>†</sup> This work was supported by The Howard Hughes Medical Institute and a Fogarty International Research Collaboration Award from the NIH. D.W.L. is a Department of Defense Air Force Laboratory Graduate Fellow.

\* To whom correspondence should be addressed.

<sup>‡</sup> The Howard Hughes Medical Institute.

<sup>§</sup> The Department of Molecular Biophysics and Biochemistry.

<sup>||</sup> Present address: Instituto de Química y Fisicoquímica Biológicas, Facultad de Farmacia y Bioquímica (UBA-CONICET), Buenos Aires, Argentina.

<sup>⊥</sup> Present address: Department of Biochemistry, Duke University Medical School, Durham, NC.

<sup>¶</sup> Present address: Department of Physiology, University of Michigan, Ann Arbor, MI.

<sup>®</sup> Abstract published in *Advance ACS Abstracts*, October 15, 1994.

<sup>1</sup> Abbreviations: EPD–Fe, (EDTA-2-aminoethyl) 2-pyridyl disulfide–Fe<sup>3+</sup>; PVDF, poly(vinylidene difluoride); GuHCl, guanidinium hydrochloride; pdTp, thymidine 3',5'-bisphosphate; HEPES, 4-(2-hydroxyethyl)-1-piperazineethanesulfonic acid; Tris, tris(hydroxymethyl)aminomethane; DTNB, 5,5'-dithiobis(2-nitrobenzoic acid); DNPH, 2,4-dinitrophenylhydrazine; TFA, trifluoroacetic acid; SEC, size exclusion chromatography. Nuclease variants are designated using the single-letter amino acid code: naming the residue changed first, then the sequence position, and finally the introduced residue.

This generates reactive oxygen species that promote localized cleavage of the protein backbone. To be appropriate for the analysis of native and nonnative protein states, a chemical cleavage technique must meet the following criteria. First, the chemical modification should not perturb the structure of the protein system. Thus the cleavage reagent should be hydrophilic to limit potentially disruptive interactions between it and exposed hydrophobic regions of nonnative proteins. Second, cleavage should occur under a variety of solution conditions where nonnative protein states can be populated at equilibrium. Third, the reagent should cleave the protein only once, as a cleaved protein fragment will have a range of conformations distinct from the state under investigation. The cleavage should occur within the protein molecule to which the reagent is attached and should ideally be predictable by simple calculations to aid in experimental design and interpretation. Fourth, and most importantly, the lifetime of the cleavage-promoting species should be short compared with the lifetime of the protein conformation under investigation. If the lifetime of the reactive species were longer than that of the protein's conformational state, the reagent would tend to oversample compact native-like conformations and provide a distorted measure of their population and conformation. If the conditions listed above are met, the technique should provide a quantitative measure of a particular protein conformational state and information concerning its structure.

Here we applied the cleavage technique to a series of nuclease variants, each with a unique cysteine residue at distinct locations on the protein surface, to assess the suitability of EPD-Fe as a probe for the quantitation and analysis of native and nonnative protein structures. Site-directed mutation and EPD-Fe modification led to only minor changes in the stability of nuclease and resulted in no detectable change in its enzymatic activity or global structure. Cleavage was obtained under a variety of solution conditions where nonnative states can be stabilized. The cleavage patterns varied with the site of EPD-Fe attachment and were dependent upon the conformation of the protein. Analysis of fragmentation for which N-terminal sequence and high-resolution mass spectrometric data were available suggests a single cleavage event per protein molecule. These data are consistent with an earlier, more extensive study of EPD-Fe-mediated peptide cleavage (Platis et al., 1993). Using the high-resolution crystal structure of nuclease as a model, we analyzed the structural basis of the cleavage patterns observed with each variant. A simple conformational analysis of the reagent in the context of the protein structure combined with the solvent accessibility of C $\alpha$  cleavage sites was successful in predicting the cleavage sites obtained for the native proteins. Most importantly, the chemical cleavage technique can be used to quantitate the denaturant-induced unfolding of nuclease, indicating that the lifetime of the reagent-generated reactive oxygen species is sufficiently short to monitor the population and structure of nonnative protein species. Thus the EPD-Fe-mediated protein cleavage technique possesses the properties necessary for the analysis of nonnative protein structures.

## EXPERIMENTAL PROCEDURES

**General Details.** Solutions of GuHCl (Mallinckrodt, GenAR) were prepared and standardized as described (Nozaki, 1972). pdTp was purchased from USB. High-

performance liquid chromatography (HPLC) was carried out with a computer-controlled system (rabbit HP; Rainin, Woburn, MA) with absorbance detection at 215 nm. Thiol groups were determined using DTNB (Ellman, 1959). Nuclease concentration was determined by absorbance measurement at 280 nm (Taniuchi & Anfinsen, 1966). Amino acid analysis was performed on a Beckman 7300 autoanalyzer. Peptides were sequenced using an Applied Biosystems 470A sequencer. SDS-PAGE was performed as described (Schägger & Von Jagow, 1987). The separating gel [16.5% T, 6% C, containing 13.3% glycerol (w/v)] was overlaid by a stacking gel (4% T, 3% C). Sample buffer was 4% SDS, 12% glycerol (w/v), 2% 2-mercaptoethanol, 0.01% Bromophenol Blue, and 50 mM Tris-HCl, pH 6.8. EPD-Fe was synthesized as described (Ermácora et al., 1992).

**Preparation and Derivatization of Single Cysteine Nuclease Variants.** Nuclease mutants were produced by PCR site-directed mutagenesis of the wild-type nuclease gene cloned into M13jg18 (Hynes et al., 1989). The construct was cloned into pAS1 under the control of  $\lambda$  P<sub>L</sub> promoter and transformed into *Escherichia coli* strain AR120. Over-expressed nuclease variants were extracted, purified, and analyzed as described (Ermácora et al., 1992).

Protein-EDTA-Fe conjugates were prepared as described (Ermácora et al., 1992). Briefly, P11C, T13C, K28C, K64C, K70C, and H124C nuclease variants were dissolved in 75 mM Tris-HCl, pH 7.2, and immediately reacted with EPD-Fe (0.75 mM protein and 1.5 mM EPD-Fe in 100- $\mu$ L total volume). The solution was incubated at room temperature for 1 h. The protein-EDTA-Fe conjugate was then purified from residual EPD-Fe and thiopyridone by spin-column chromatography (Penefsky, 1979) using Bio-Gel P2 (100–200 mesh, Bio-Rad) equilibrated in 75 mM reaction buffer. The extent of the coupling reaction was determined by titrating the residual free thiol group with DTNB (Ellman, 1959).

**Cleavage Reaction.** The standard cleavage reaction was carried out for 30 min at 23 °C in either 50 mM HEPES, pH 7.0, or 100 mM Tris-HCl, pH 7.2, with a protein concentration of 15  $\mu$ M. The reaction was initiated by adding ascorbate (adjusted to pH 7.0 with NaOH) to give a final concentration of 20 mM. Unless otherwise indicated, the reaction was terminated by adding 2-mercaptoethanol to give 4% (v/v) final solutions. Samples for SDS-PAGE analysis were frozen (–70 °C), freeze-dried, dissolved in SDS-PAGE sample buffer, heated for 10 min at 56 °C, and electrophoresed. Samples for HPLC size-filtration analysis were brought to 3 M GuHCl and 4% (v/v) 2-mercaptoethanol, heated for 10 min at 56 °C, and chromatographed. Cleavage at pH 4.0–9.0 was performed in a buffer mixture of 30 mM CAPS, 30 mM phosphoric acid, and 30 mM acetic acid adjusted to the required pH with NaOH. When indicated, 10 mM CaCl<sub>2</sub> and 1 mM pdTp, 0.5 M mannitol, 0.5 M thiourea, or 1 mM H<sub>2</sub>O<sub>2</sub> was included in the standard reaction buffer.

**Assay for Protein Oxidation.** The standard cleavage reaction and a reaction blank were prepared using 0.5 mg each of EPD-modified nuclease H124C. The reactions were quenched with 4% (v/v) 2-mercaptoethanol, frozen, and lyophilized. The protein was dissolved in 40  $\mu$ L of 12% SDS. One and one-half volumes of 10% trifluoroacetic acid (TFA) and two volumes of 10 mM 2,4-dinitrophenylhydra-

zine (DNPH) in 10% TFA were added. The solution was allowed to react at room temperature for 30 min and then stopped with 1.5 volumes of 2 M Tris-HCl in 30% glycerol. The protein was then purified from free DNPH using spin-column chromatography (Penefsky, 1979) with Bio-Gel P4 (fine, Bio-Rad). The absorbance at 276 and 370 nm was used to calculate the moles of carbonyl per mole of protein using molar extinction coefficients of 22 000 at 370 nm and 9460 at 276 nm for hydrazones (Levine et al., 1994) and 15 300 at 276 nm for nuclease.

**Cleavage Product Characterization.** Protein fragments were partially purified by size-filtration chromatography on a HPLC column (Bio-Sil SEC250, 600  $\times$  7.5 mm, Bio-Rad). Elution buffer was 1.5 M GuHCl and 0.1 M sodium phosphate, pH 6.0, and the flow was 0.5 mL/min. Fractions from the size-filtration analysis were injected into a C<sub>18</sub> reverse-phase HPLC column (Vydac, 4.6  $\times$  250 mm). A linear gradient (1% B/min) between solvent A (0.06% TFA) and solvent B (0.05% TFA in acetonitrile) was used, and the flow was 1 mL/min. SDS-PAGE and blotting onto PVDF membranes (Matsudaira, 1987) were used to isolate some fragmentation products. Isolated peptides were characterized by N-terminal sequencing and mass spectrometry.

**Mass Spectrometry.** Electrospray mass spectra were acquired on a VG BioTech/Fisons (Altrincham, U.K.) triple-quadrupole instrument with an electrospray ionization source (Analytica, Branford, CT). The ion source was at 3.2 kV. The instrument was scanned from  $m/z$  500 to 1500 or from 1000 to 2000 in 8 s; 15 scans were acquired for each sample. Horse heart myoglobin, average mass 16 951.5 Da (Sigma Chemical Co., St. Louis, MO), was used as the standard for instrument calibration. Typically, samples in 50% methanol and 1% acetic acid were introduced into the spectrometer at 0.3  $\mu$ L/min with a 2  $\mu$ L/min 1- or 2-propanol sheath.

**Fluorescence Measurement.** F3010 Hitachi (Hitachi Ltd., Tokyo, Japan) or Spex Fluoromax (Spex Industries, Edison, NJ) fluorometers were used; all measurements were made at 23 °C. Excitation wavelength was at 295 nm and emission was recorded at 320 nm (Eftink et al., 1991). The protein concentration was 3  $\mu$ M in 50 mM HEPES, pH 7.0, with or without 10 mM CaCl<sub>2</sub> and 0.5 mM pdTp. GuHCl unfolding transitions were monitored by adding the denaturant to the protein sample from a 6 M stock solution in the corresponding buffer and allowing for equilibration for 10 min before a new reading of fluorescence was recorded. The unfolding reaction was essentially complete after the equilibration. Appropriate correction for protein dilution was introduced in the calculations. The apparent free energy of unfolding was calculated as described (Eftink et al., 1991). SigmaPlot software (Jandel Scientific, San Raphael, CA) was used to perform the nonlinear fitting of the data.

**Circular Dichroism Spectroscopy.** Circular dichroism (CD) spectra were obtained with an Aviv Circular Dichroism DS-60 spectropolarimeter at 25 °C in 2.5 mM HEPES and 50 mM KF, pH 7.0. The cuvette path length was 0.1 cm, and the protein concentration was typically 10  $\mu$ M. Data were collected for 1 s every 0.5 nm with a 1.5-nm bandwidth. The average of seven scans was recorded for each sample, and the average spectra were smoothed using a fourth-order polynomial function and a ten-point window. Two spectra for each sample were averaged and plotted.

**Enzymatic Activity Measurements.** The hydrolysis of denatured DNA was followed by the hyperchromic absor-

bance effect at 260 nm. The reaction was performed essentially as described by Cuatrecasas et al. (1967). Briefly, the initial velocity of hydrolysis was determined at 23 °C with a saturating concentration of substrate. Reaction buffer was 50 mM Tris-HCl and 10 mM CaCl<sub>2</sub>, containing 50  $\mu$ g/mL heat-denatured salmon sperm DNA (Sigma Chemical Co., St. Louis, MO), pH 8.8. Nuclease stock solutions were prepared in 50 mM HEPES, pH 7.0, containing 1 mg/mL bovine serum albumin to diminish nonspecific absorption to tubes and cuvettes; typically, 10  $\mu$ L of solution was added to 1 mL of reaction buffer, yielding a final nuclease concentration of 0.01  $\mu$ g/mL. Nuclease specific activity is given in units per milligram. One unit of nuclease activity is the amount of enzyme causing an absorbance change at 260 nm of 1.0 per minute.

**Monitoring the Unfolding of H124C-EDTA-Fe by the Yield of the 1-102 Cleavage Product.** The standard cleavage reaction was carried out in 50 mM HEPES, pH 7.0, containing 0-2 M GuHCl and, when indicated, 10 mM CaCl<sub>2</sub> and 0.5 mM pdTp. Samples containing the same amount of protein were analyzed by denaturing HPLC size-exclusion chromatography with absorbance detection at 215 nm (see above). A Perkin-Elmer ISS-100 autosampler was used to inject equal sample volumes. Dynamax (Rainin, Woburn, MA) software was used for data acquisition and processing. The area corresponding to each fragmentation product was recorded as a percentage of the total area of the reaction products. The extent of cleavage at position 102 (Figure 5C, peak b) as a function of denaturant was normalized to the cleavage yield at 0 M GuHCl (folded state). Cleavage at position 102 in 2 M GuHCl was negligible. Curves were fitted to the data by inspection.

**Conformational Modeling of Nuclease-EDTA-Fe.** A conformational analysis of the EDTA-Fe reagent attached to each cysteine site examined experimentally was carried out using the DEZYMER program (Hellenga & Richards, 1991). A model of the EPD adduct was prepared from the crystal structure of staphylococcal nuclease (Hynes & Fox, 1991) and a model of EPD based on the crystal structure of EDTA-Fe. The conformations of the reagent without internal van der Waals clashes were determined at the  $t$ ,  $g^+$ , and  $g^-$  rotamers for single bonds,  $+90^\circ$  and  $-90^\circ$  for the disulfide, and at  $15^\circ$  intervals for the bonds preceding and following the amide linkage of the tether ( $\chi_6 -180^\circ$  to  $180^\circ$  and  $\chi_7 -60^\circ$  to  $105^\circ$ ). The  $\chi_8$  angle could only adopt the  $g^-$  conformation. A total of 18 698 conformations were found to be free of internal clashes. A discrete conformational tree search was computed for each nuclease-EDTA-Fe adduct using the predefined allowed conformations for the reagent. Reagent conformations were excluded from further consideration if any atom of the reagent clashed with one or more atoms of the protein crystal structure. An attempt was made to relieve an observed clash by testing conformations displaced  $\pm 10^\circ$  from the last sampled ideal rotamer angle. The position of the Fe atom and of a coordinated water molecule used as a model for the site of hydroxyl radical formation was recorded. Statistics concerning the conformation search are presented in Table 3. A relatively small fraction of the conformers was excluded, consistent with the highly exposed surface location of the cysteine attachment sites. The distribution of distances between Fe and C $\alpha$  was calculated for each protein C $\alpha$ , using DEZYMER. The histograms were plotted using EXCEL for

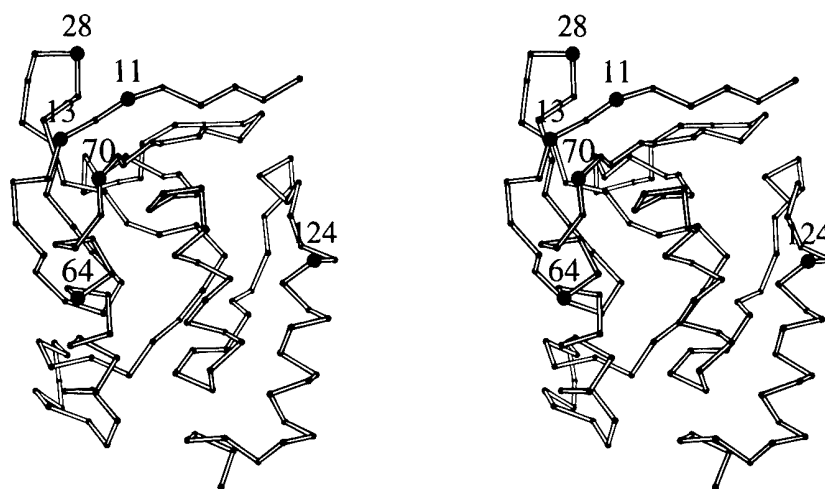


FIGURE 1: Stereo diagram of a staphylococcal nuclease C $\alpha$  trace with the positions of the single cysteine substitutions used in this study indicated by large filled spheres.

an Apple Macintosh computer. Solvent accessibility calculations were carried out as defined by Lee and Richards (1971). The Fe probability distribution was calculated by counting all Fe sites within 0.5 Å of a 1.0-Å cubic lattice. The resulting distributions were contoured and displayed with Insight II (Biosym, San Diego, CA).

## RESULTS

**Preparation and Characterization of Protein-EDTA-Fe Conjugates.** The residues replaced by cysteine in each mutant were selected by inspection of the three-dimensional structure of wild-type nuclease (Hynes & Fox, 1991). Surface residues that do not form hydrogen bonds and van der Waals interactions with the remainder of the protein were selected as possible cysteine substitution sites. Further, surface residues were selected as cysteine substitution sites only if, after reaction with EPD, they would allow the modeled EDTA-Fe moiety to come close to segments of the protein structure well separated in amino acid sequence. Six single-cysteine variants of staphylococcal nuclease (P11C, T13C, K28C, K64C, K70C, H124C) were constructed by site-directed mutagenesis. The P11C- and T13C-EDTA-Fe attachment sites are both on an extended  $\beta$ -strand separated by one intervening residue (distance C $\alpha$ 11-C $\alpha$ 13 = 7.0 Å) and thus project in a common orientation (Figure 1). These attachment sites were chosen to examine the range of cleavage sites accessible to reagent-generated reactive oxygen species. The K28C substitution is within a  $\beta$ -turn separating the second and third  $\beta$ -strands. The reagent projects across the twisted  $\beta$ -sheet and is close to  $\beta$ -strand 1 and an extended loop connecting  $\beta$ -strands 4 and 5. The K64C site is within  $\alpha$ -helix 1 and close to  $\alpha$ -helix 2 that runs parallel and adjacent to it. The K70C site is in an extended segment connecting helix 1 and  $\beta$ -strand 4 and is in proximity to  $\beta$ -strand 1. The H124C site is within  $\alpha$ -helix 3 that is parallel and adjacent to  $\alpha$ -helix 2. Each purified protein contained 1.0 cysteine residue per molecule as determined by the DTNB reaction (Ellman, 1959) and had the correct mass to within  $\pm 0.01\%$  as determined by electrospray ionization mass spectrometry.

Nuclease variants were modified with EPD-Fe. This reagent promotes the attachment of an EDTA-Fe complex to the cysteine residues through a disulfide bridge (Ermácora

Table 1: Nuclease Activity Assay<sup>a</sup>

protein variant	activity <sup>b</sup> $\pm$ SD	no. of determinations
wild type	1.00 $\pm$ 0.08	14
P11C-EDTA-Fe	0.99 $\pm$ 0.11	6
T13C-EDTA-Fe	1.02 $\pm$ 0.17	6
K28C-EDTA-Fe	1.07 $\pm$ 0.13	6
K64C-EDTA-Fe	1.03 $\pm$ 0.02	3
K70C-EDA-Fe	1.12 $\pm$ 0.16	6
H124C-EDTA-Fe	1.07 $\pm$ 0.02	3

<sup>a</sup> The assay was performed as described (Cuatrecasas et al., 1967).

<sup>b</sup> As a fraction of wild-type activity (3999 units/mg).

et al., 1992). Titration of free thiol groups and polyacrylamide gel electrophoretic analysis under nonreducing conditions demonstrated a modification yield greater than 95%. Protein-protein disulfide formation was negligible as shown by SDS-PAGE.

The surface cysteine replacements and subsequent modification with EPD-Fe might affect the structure, function, or stability of the protein, compromising the interpretation of the cleavage results. All modified proteins were analyzed by a number of techniques to assess their similarity to the wild-type protein as described below.

The enzyme activity of a protein is often the most sensitive probe of native structure. Under conditions of saturating substrate, all nuclease-EDTA-Fe conjugates had full enzymatic activity (Table 1). Wild-type nuclease was used as the standard for the measurement and had a specific activity of 3999 units/mg, which is slightly higher than recently reported (Shortle & Meeker, 1989).

Derivatization of the cysteine variants with EPD-Fe did not significantly alter the apparent secondary structure of the protein, as judged by the superposability of the CD spectra in the far-UV region (Figure 2). The thermodynamic stability of the cysteine variants, and the corresponding EDTA-Fe derivatives, was determined by equilibrium unfolding titration of the tryptophan fluorescence using GuHCl as the denaturant. The free energy and other related parameters for the unfolding reaction are shown in Table 2. These results indicate that modified nucleases are stable and fully folded in the absence of denaturant. The cysteine substitution and chemical modification caused modest changes in the free energy of unfolding of most protein variants. All the mutations but one destabilized the protein by 0.3–0.9

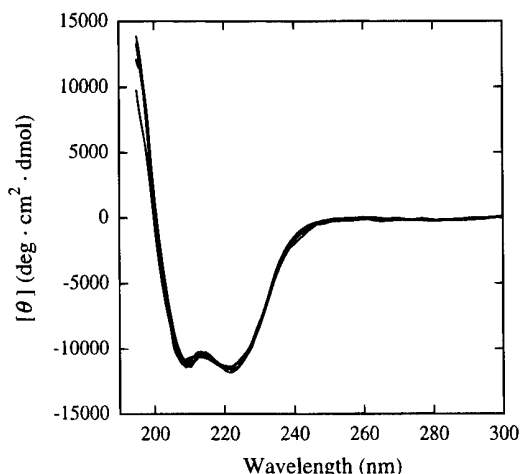


FIGURE 2: CD spectra of wild-type nuclease and nuclease-EDTA-Fe variants. Analysis was performed at 25 °C in 2.5 mM HEPES and 50 mM KF, pH 7.0. The spectra of wild-type nuclease and the nuclease-EDTA-Fe adduct of P11C, T13C, K28C, K64C, K70C, and H124C were superimposed in a single graph to highlight the similarity of the traces.

Table 2: Free Energy Change and Other Related Parameters for the GuHCl Unfolding of Nuclease Variants and Their EDTA-Fe Adducts<sup>a</sup>

protein	$\Delta G_{un}^{\circ}$ (kcal/mol)	$m$ (kcal/mol·M)	$C_m$ (M) <sup>b</sup>
wild type	$4.67 \pm 0.18$	$6.38 \pm 0.16$	0.73
P11C	$4.13 \pm 0.12$	$6.79 \pm 0.20$	0.61
P11C-EDTA-Fe	$4.00 \pm 0.11$	$6.45 \pm 0.17$	0.62
T13C	$4.37 \pm 0.19$	$7.44 \pm 0.32$	0.59
T13C-EDTA-Fe	$3.79 \pm 0.33$	$5.79 \pm 0.49$	0.65
K28C	$4.23 \pm 0.13$	$7.18 \pm 0.22$	0.59
K28C-EDTA-Fe	$2.36 \pm 0.04$	$5.44 \pm 0.08$	0.43
K64C	$3.81 \pm 0.15$	$6.19 \pm 0.24$	0.61
K64C-EDTA-Fe	$5.05 \pm 0.32$	$6.73 \pm 0.43$	0.75
K70C	$4.21 \pm 0.19$	$7.07 \pm 0.30$	0.59
K70C-EDTA-Fe	$4.06 \pm 0.11$	$5.99 \pm 0.16$	0.68
H124C	$4.50 \pm 0.12$	$6.53 \pm 0.17$	0.69
H124C-EDTA-Fe	$4.68 \pm 0.25$	$6.64 \pm 0.35$	0.82
H124C-EDTA-Fe <sup>c</sup>	$6.49 \pm 0.41$	$6.17 \pm 0.39$	1.05

<sup>a</sup> Unfolding experiments were conducted at 23 °C in 50 mM Hepes, pH 7.0.  $\Delta G_{un}^{\circ}$  and  $m$  were calculated as described (Eftink et al., 1991). Standard deviations were obtained from the fitting program (see Experimental Procedures). To estimate the interassay error, triplicate measurement of wild-type protein was performed:  $\Delta G_{un}^{\circ} = 4.60 \pm 0.15$ ;  $m = 6.31 \pm 0.60$ . <sup>b</sup> The GuHCl concentration that causes 50% unfolding was calculated as  $\Delta G_{un}^{\circ}/m$ . <sup>c</sup> In the presence of 10 mM  $Ca^{2+}$  and 1 mM pdTp.

kcal/mol; the free energy of unfolding of the H124C variant was indistinguishable from that of the wild-type protein. The subsequent EPD-Fe modification did not affect the stability of P11C, K70C, or H124C but did further lower the stability of T13C and K28C. Notably, the attachment of the EDTA-Fe moiety restored the stability of K64C to the wild-type value. The combined effect of mutation and chemical modification resulted in nuclease-EDTA-Fe variants that were less stable than the wild type by 0.4–0.9 kcal/mol, with the exception of K28C-EDTA-Fe which was 2.3 kcal/mol less stable and H124C-EDTA-Fe which was not significantly different from the wild-type protein.

**Cleavage Reaction.** The cleavage reaction of EPD-Fe-modified nuclease variants was initiated with the addition of 20 mM ascorbate and analyzed by SDS-PAGE (Figure 3). In all cases the procedure resulted in polypeptide backbone cleavage. At least four or five major cleavage sites

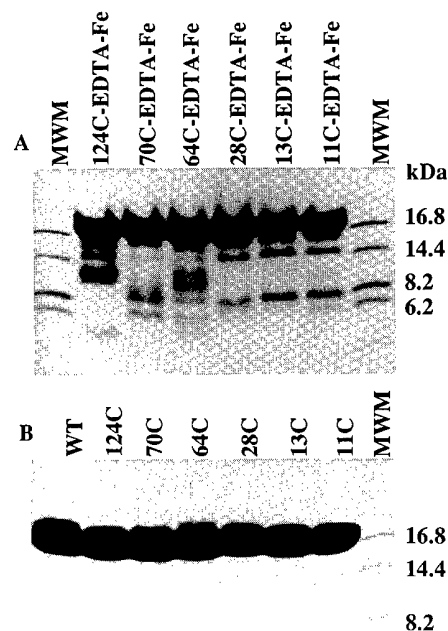


FIGURE 3: SDS-PAGE analysis of nuclease-EDTA-Fe cleavage products. Panel A: The indicated protein variants after the reaction with ascorbate (see Experimental Procedures). Panel B: The corresponding unmodified nuclease single cysteine variants.

were obtained for each protein. The yield of the cleavage reaction varied from 1–2% for K28C-EDTA-Fe to approximately 15% for H124C-EDTA-Fe. A distinct fragmentation pattern of the polypeptide backbone for each variant was obtained except for P11C-EDTA-Fe and T13C-EDTA-Fe, which were very similar, consistent with the close proximity and relative orientation of these two attachment sites.

P11C-EDTA-Fe, K64C-EDTA-Fe, and K70C-EDTA-Fe were also subjected to the cleavage reaction in the presence of 10 mM  $CaCl_2$  and 1 mM pdTp or in 4.8 M urea (Figure 4). As a control, 4% 2-mercaptoethanol was added at time 0 to quench the reaction before the addition of ascorbate (Figure 4, lanes 1). No cleavage was observed in these reaction blanks. The addition of  $Ca^{2+}$  and pdTp, which are nuclease ligands that stabilize the folded state by approximately 2 kcal/mol under these conditions (see below), has no apparent effect on the native cleavage pattern (compare lanes 2 and 3 in Figure 4). In the presence of 4.8 M urea (within the unfolded baseline of nuclease), strong cleavage bands were observed with electrophoretic mobilities consistent with polypeptide cleavage at sites close in sequence to the cysteine bearing the EDTA-Fe complex, while the cleavage bands generated under native conditions were no longer observed. A few weak bands whose mobility does not correspond to local cleavage products were present even in 4.8 M urea, suggesting some residual long-range interactions may be present.

H124C-EDTA-Fe was cleaved under the conditions described above, and the cleavage products were analyzed by size-exclusion HPLC under denaturing conditions (Figure 5). The elution profiles indicated that the cleavage pattern was different when the cleavage reaction was conducted under native conditions and under nonnative conditions in the presence of denaturants (compare panels C and D in Figure 5). Again, the results indicate that the cleavage products result from long-range interactions in the folded

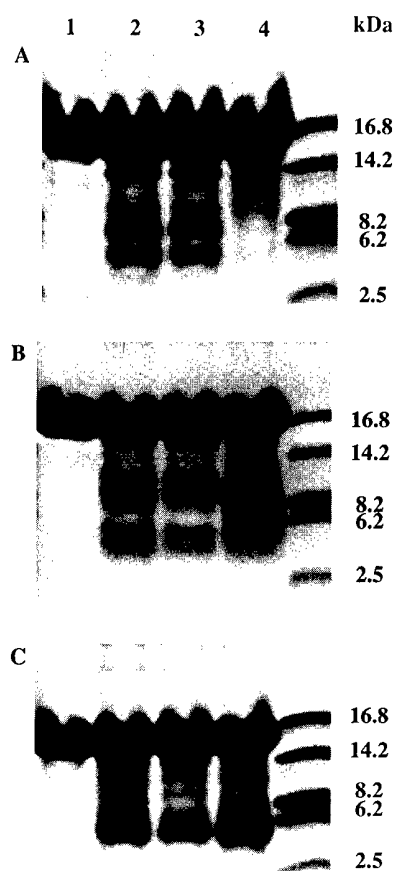


FIGURE 4: SDS-PAGE analysis of the conformation dependence of the cleavage products. Panel A, B, and C correspond to P11C-EDTA-Fe, K64C-EDTA-Fe, and K70C-EDTA-Fe, respectively. Lanes 1: Blanks, the reaction was stopped at time 0 by adding 4% 2-mercaptoethanol before ascorbate. Lanes 2: Standard cleavage reaction (see Experimental Procedures). Lanes 3: Cleavage reaction in the presence of 10 mM  $\text{CaCl}_2$  and 1 mM pdTp. Lanes 4: Cleavage reaction in the presence of 4.8 M urea. Unlabeled lanes: Molecular weight markers.

state that are disrupted by denaturants. The addition of  $\text{Ca}^{2+}$  and pdTp had no effect on the native cleavage reaction product pattern (not shown).

**Identification of Cleavage Sites.** The fragmentation products were purified using size-exclusion and reverse-phase HPLC or SDS-PAGE followed by electroblotting onto PVDF membranes. The purified peptides were sequenced and, in some cases, characterized by mass spectrometry. The sites of cleavage identified for each protein variant are shown in Table 3 along with the analytical data that led to their characterization. For the five cysteine variants analyzed, 26 cleavage sites were identified. Cleavage sites for the H124C-EDTA-Fe variant in the GuHCl-induced unfolded state were also characterized. Cleavage site data for K28C-EDTA-Fe are from a previous study (Ermácora et al., 1992) and are included here for completeness.

The chemical characterization of the cleavage sites confirmed what was previously predicted on the basis of the mobility of the reaction products in SDS-PAGE. Two types of cleavage sites were observed, local cleavage arising from sequential proximity that involved residues at  $n - 6$  to  $n + 7$  positions at both sides of the reagent attachment sites and cleavage sites due to long-range interactions that involved residues well separated in sequence from the reagent attach-

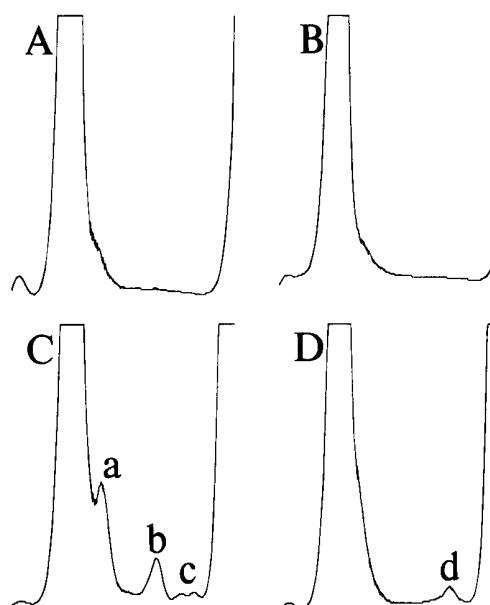


FIGURE 5: Size exclusion analysis of the H124C-EDTA-Fe cleavage reaction products. The cleavage reaction was started by the addition of ascorbate as described in Experimental Procedures. The reaction was terminated after 30 min by incubation with 1.5 M GuHCl and 4% 2-mercaptoethanol (15 min at 65 °C) and injected into the HPLC system with an absorbance detector set at 215 nm. The shown traces start at the elution time corresponding to approximately 40 kDa, include the uncleaved nuclease peak (16.8 kDa), and end when ascorbate and other low molecular weight components of the reaction mixture start to elute. Panel A: Reaction blank; no ascorbate was added. Panel B: The reaction was quenched at time 0 by 2-mercaptoethanol (4% final concentration added before the ascorbate). Panel C: Cleavage reaction. Panel D: Reaction performed in the presence of 1.5 M GuHCl. Peaks a-c, (panel C) and d (panel D) were isolated for further analysis.

ment site but brought into close proximity by the fold of the protein.

The cleavage reaction seems independent of the nature of the amino acid side chain. Data collected in Table 3 show that 10 of 20 amino acid types occurring in the nuclease sequence were cleaved. Hydrophobic and hydrophilic, charged and uncharged amino acid side chains are represented in the collection of cleavage sites. Lysine is the single most abundant residue involved in a cleavage event; however, lysine is also the most abundant residue in nuclease (21 of 149), all occurring at the protein surface. The number of cleavage sites observed is too small to determine a statistically significant reaction preference toward a particular side chain.

The position of the EPD-Fe attachment site and the sites of cleavage were mapped on an  $\alpha$ -carbon trace for each variant (Figure 6). The cleavage sites cluster in a region of the molecular surface surrounding each cysteine reagent attachment site. A set of cleavage sites are shared by C11 and C13 (Figure 6A,B), consistent with their proximity in sequence and common  $\text{C}\alpha$ - $\text{C}\beta$  bond orientation. There is a structural reciprocity in the cleavage experiments. When the reagent was attached to one secondary structural element ( $\beta$ -strand 1: C11 and C13), it cleaved at a neighboring element ( $\beta$ -turn 2: K28 and G29) (Figure 6A,B). When the reagent was attached to the second element ( $\beta$ -turn 2: C28), cleavage was observed in the first element ( $\beta$ -strand 1: H8) (Figure 6C).

When the reagent was attached to a residue within an  $\alpha$ -helix, cleavage was observed on the solvent-exposed face

Table 3: Products of the Nuclease-EDTA-Fe Cleavage Reaction<sup>a</sup>

fragments from	PAGE or SEC <sup>b</sup> (kDa)	N-terminal sequence <sup>c</sup> or measured mass <sup>d</sup>	assignment <sup>e</sup> and calcd mass values	cleavage sites	solvent accessibility <sup>f</sup> (Å <sup>2</sup> )	distance to closest Fe position <sup>g</sup> (Å)
H124C-EDTA-Fe (folded state)	11-12	1-11				
		11407.8 ± 4.2 <sup>h</sup>	1-102 (11406.4)	A102	2.8	6.9
		11430.1 ± 6.6 <sup>i</sup>	1-102 (11436.3)	A102	2.8	6.9
		13551.7 ± 7.4	1-121 (13551.2)	H121	1.9	4.4
	7965 <sup>j</sup>	13711.6 ± 8.5	1-122 (13710.3)	E122	0.0	6.4
	14	1-16				
	13	1-16				
	10	1-5				
	9	1-5				
	5-6	103-132	103-149 (5361.0)	A102		
	2-3	128-138	128-149 (2449.6)	K127	3.8	5.6
		132-137	132-149 (2034.2)	Q131	0.1	9.5
H124C-EDTA-Fe (unfolded state)	14-15	1-5	[1-127] [1-129]			
	2-3	128-137	128-149 (2449.6)	K127		
		130-139	130-149 (2233.4)	E129		
K70C-EDTA-Fe	7-10	65-75	65-149 (9690.9)	K64	3.9	10.1
		66-78	66-149 (9559.7)	M65	7.8	10.0
		70-75	70-149 (9146.3)	A69	2.1	6.1
		72-84	72-149 (8915.0)	K71	7.4	4.6
	7-10	73-85	73-149 (8801.8)	172	0.0	7.4
		1-11	[1-72] [1-65] [1-71]			
K64C-EDTA-Fe	7-10	1-8				
	5-6	103-115	103-149 (5395.0)	A102	2.8	9.2
	4048 <sup>j</sup>	12	1-11			
	9	1-11				
		61-69	61-149 (10195.6)	A60	3.1	5.3
		72-82	72-149 (8915.0)	K71	7.4	13.9
	6	103-113	103-149 (5395.0)	A102	2.8	9.2
	5	106-114	106-149 (5026.5)	R105	0.0	10.3
		98-108	98-149 (5939.7)	K97	6.1	10.8
K28C-EDTA-Fe	16	9-19		H8	3.5	7.0
	6-8	72-82		K71	7.4	16.5
		79-89		K78	5.5	6.4
		81-91		Q80	11.1	5.7
		85-95		K84	13.3	12.5
	15	16-26	16-149 (15192.4)	115	4.4	5.6
	13	29-38	29-149 (13728.6)	K28	14.3	6.1
		30-38	30-149 (13671.6)	G29	38.3	5.9
T13C-EDTA-Fe	15	72-83	72-149 (8915.0)	K71	7.4	5.8
	7	1-10				
	6	1-10				
P11C-EDTA-Fe	15	16-26	16-149 (15192.4)	115	4.4	11.3
	7874 <sup>j</sup>	29-39	29-149 (13728.6)	K28	14.3	4.6
		30-38	30-149 (13671.6)	G29	38.3	4.9
		1-9				
	10	65-74	65-149 (9716.0)	K64	3.9	16.8
	8	72-82	72-149 (8915.0)	K71	7.4	5.4
		73-82	73-149 (8801.8)	172	0.0	6.9
		1-7				
	6	1-10				

<sup>a</sup> Cleavage experiments were performed as described under Experimental Procedures. Reaction products were isolated by HPLC (size exclusion chromatography under denaturing conditions followed by reverse-phase chromatography) or by SDS-PAGE and blotting onto PVDF membranes. Isolated products were subjected to sequential Edman degradation. <sup>b</sup> Apparent molecular weight based on electrophoretic mobility (single numbers) or on the elution time on the size exclusion separation (range). <sup>c</sup> Residues corresponding to the nuclease sequence. <sup>d</sup> Analysis performed by electrospray ionization mass spectrometry. <sup>e</sup> An assignment was made when the fragment was sequenced and gave an N-terminal residue different from residue 1 in the nuclease sequence. Tentative assignments are shown between brackets. <sup>f</sup> Calculated according to Richards (1977) using a sphere of radius 1.4 Å. <sup>g</sup> Distance between the Cα and the closest iron position. <sup>h</sup> Product formed by oxidation as in Figure 9d. <sup>i</sup> Product formed by oxidation (Figure 9c) or by hydrolytic cleavage (Figure 9b). <sup>j</sup> Number of allowed conformers determined by rotamer calculation.

of that α-helix one and two turns away. Cleavage of K64C-EDTA-Fe occurred one turn away at A60 (Figure 6D), while for H124C-EDTA-Fe cleavage occurs at K127 and Q131, one and two turns away, respectively. The proximity of α-helices 1 and 2 was monitored by K64C-EDTA-Fe (helix 1) with cleavage at Ala102 and Arg105, one turn away (helix 2) (Figure 6D). Likewise, the proximity of α-helices 2 and 3 was monitored by H124C-EDTA-Fe (helix 3) with cleavage again at Ala102. Only local cleavage sites have

so far been characterized for K70C-EDTA-Fe (Figure 6E, Table 3) although low-yield cleavage products are seen on SDS gels which must arise from long-range interactions (Figure 4C).

The surface exposure of the cleavage sites was examined using the solvent accessibility algorithm of Lee and Richards (1971) and is reported in Table 3. The sites of cleavage generally have an accessible surface area of >3 Å<sup>2</sup> for Cα (Table 3) (the site of oxidative cleavage, see below) while

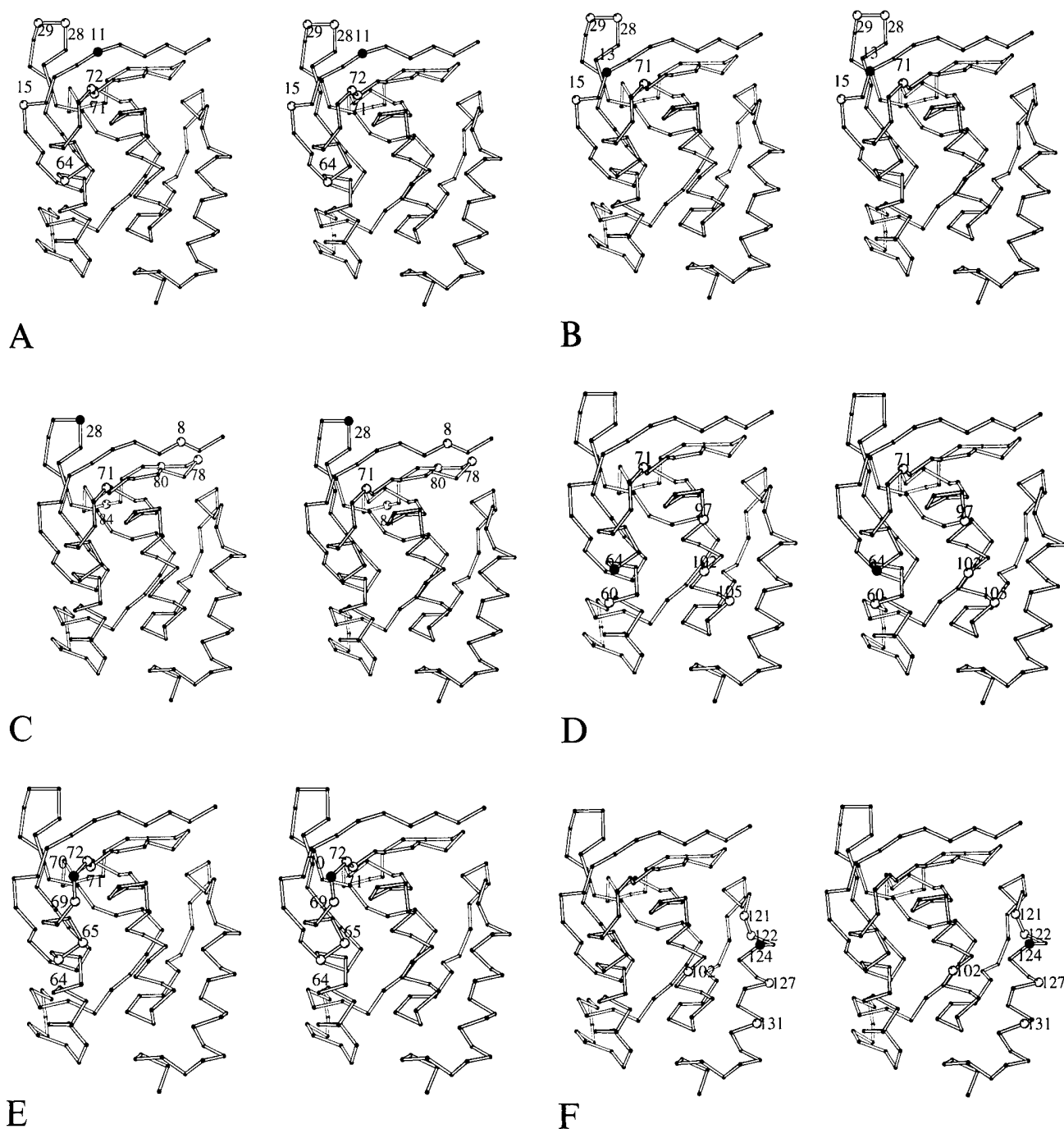


FIGURE 6: Stereo diagram of a staphylococcal nuclease C $\alpha$  trace with the positions of the cysteine site of attachment indicated by a large filled sphere and the cleavage sites indicated by large gray spheres: (A) P11C, (B) T13C, (C) K28C, (D) K64C, (E) K70C, and (F) H124C.

the carbonyl carbon (the site of hydrolytic cleavage) generally has zero accessible surface area (data not shown). Some of the observed cleavage sites have zero accessible surface area for C $\alpha$ ; however, visual inspection of the structure indicates that these sites are at the protein surface and could be exposed to the solvent probe by the reorientation of a side chain or by modest conformational fluctuations about the average crystallographic structure.

**Nature of the Chemical Cleavage Reaction.** A number of aspects of the chemical cleavage reaction were investigated to optimize the technique and to better understand the chemistry involved and the range of solution conditions in which the method can be applied. H124C-EDTA-Fe was selected for this purpose because upon cleavage it gives a high-yield peak in size-exclusion HPLC analysis which was

amenable to precise quantitation (see Figure 5, panel C, peak b). This peak corresponds to residues 103–149 of the nuclease sequence (Table 3), indicating that cleavage occurred at residues 102 and 105. Residues 102 and 124 (the site of attachment of EDTA-Fe) are located in two adjacent helices (H2 and H3, respectively) separated by 11.34 Å (distance C $\alpha$ 102–C $\alpha$ 124) in the native fold of the protein (Hynes & Fox, 1991; Figure 6F).

The time course of the reaction at 23 and 4 °C is shown in Figure 7. The reaction is only slightly slower at 4 °C, and it is almost complete after 30 min at both temperatures. The initial rate of the reaction was accelerated by 1 mM H<sub>2</sub>O<sub>2</sub>, indicating that hydrogen peroxide generation by the Fe-ascorbate system is involved in the cleavage mechanism.

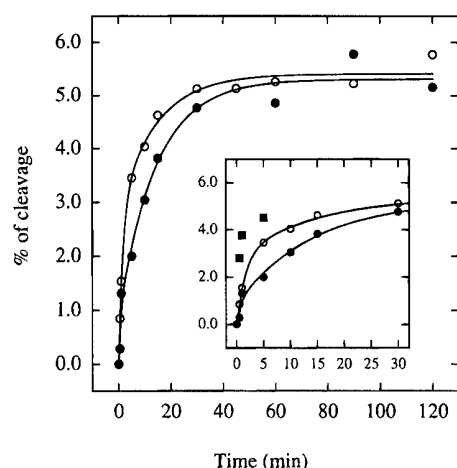


FIGURE 7: Kinetic analysis of the H124C-EDTA-Fe cleavage reaction. The area under peak b (Figure 5C) was used to quantitate the yield of the reaction. This cleavage product maps cleavage at residue 102. Temperature: (○) 23 °C; (●) 4 °C. Insert: (■) reaction in the presence of 1 mM H<sub>2</sub>O<sub>2</sub>.

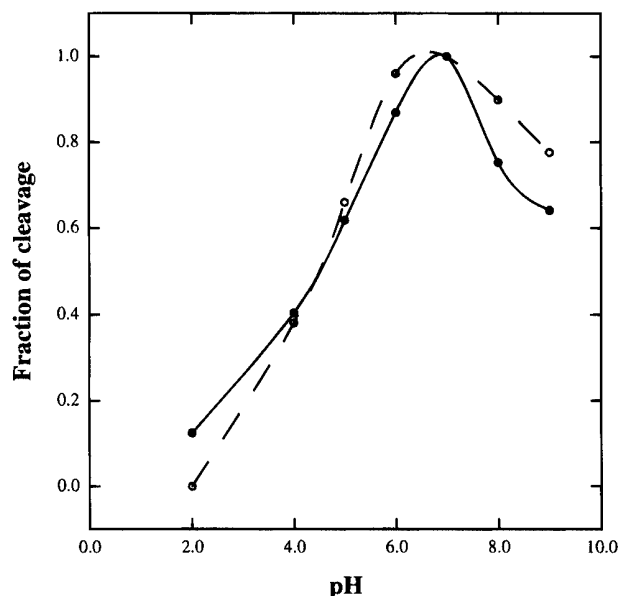


FIGURE 8: pH dependence of the H124C-EDTA-Fe cleavage reaction. Filled circles indicate the yield of nuclease fragment 1-102 (Figure 5C, peak a) and are connected with a solid line. The open circles indicate the yield of nuclease fragment 103-149 (Figure 5C, peak b) and are connected by a dashed line.

The pH dependence of the H124C-EDTA-Fe cleavage reaction is shown in Figure 8. The yield of the cleavage is maximal near pH 7.0 and decreases at higher and lower pH. At pH 2.0, the chromatographic profile was indistinguishable from the reaction blank. Although the protein will exist in a nonnative state at pH 2.0, a distinct cleavage pattern would be expected, similar to that observed in the denatured state (Figure 5D, Table 3) if cleavage occurred. As the cleavage pattern resembled the blank, the reaction must be inhibited at pH 2.0, perhaps due to the protonation of the EDTA moiety and dissociation of the iron.

The addition of free radical scavengers is frequently used to identify the role of hydroxyl radicals in cleavage chemistry. The cleavage reaction was not inhibited by 0.5 M mannitol, and 0.5 M thiourea caused only 20% inhibition (not shown). Since both compounds are potent scavengers of hydroxyl radicals, the lack of inhibition could indicate

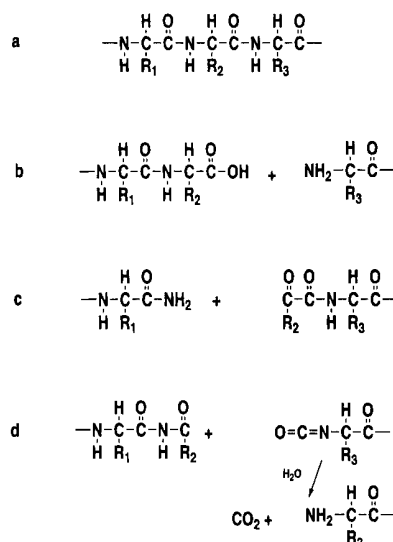


FIGURE 9: Cleavage products of a polypeptide backbone (a) resulting from (b) hydrolytic cleavage, as proposed by Rana and Meares (1991), (c) the oxidative mechanism cited by Hoyer et al. (1990), and (d) the mechanism proposed for EPD-Fe cleavage of peptides by Platis et al. (1993).

that hydroxyl radicals are not responsible for the cleavage; however, the local concentration of hydroxyl radicals at the protein surface could be much higher than that of the added scavenger. Further, negative binding or differential exclusion of solutes from the protein surface is known to occur (Timasheff & Arakawa, 1989), and this can decrease the effective concentration of the free radical scavenger at the protein-solvent interface. A similarly high concentration of mannitol did not protect glutamine synthetase from site-specific, iron-mediated fragmentation in the presence of oxygen and dithiothreitol (Kim et al., 1985). Alternatively, the reactive oxygen radical could remain bound to the iron and would thus have a high effective concentration at the protein surface.

The reaction is completely inhibited by 4% 2-mercaptoethanol (Figure 4, lanes 1, and Figure 5, panel B). Thiol compounds at low concentration can serve as an iron reductant, replacing ascorbate in sustaining the Fe-mediated production of reactive oxygen species. At higher concentration, thiols are powerful scavengers for hydroxyl radicals and could coordinate the Fe center inhibiting the generation of reactive oxygen species. Either of these two mechanisms could be responsible for the observed inhibition of the protein cleavage reaction. The same behavior of thiol compounds has been reported for DNA cleavage by EDTA-Fe-generated hydroxyl radicals. At low concentration the DNA cleavage reaction is promoted while at high concentration the reaction is inhibited (Hertzberg & Dervan, 1984).

**Cleavage Reaction Mechanisms.** The mechanism of protein cleavage mediated by the EPD-Fe reagent has been investigated using a small EPD-Fe-modified peptide (Platis et al., 1993). Two oxidative mechanisms and one hydrolytic mechanism were proposed on the basis of the chemical structure of the cleavage products shown in Figure 9. The relatively high yield of the H124C-EDTA-Fe cleavage products allowed further characterization of fragment 1-102. Electrospray mass spectrometry (Table 3) showed that this peptide was generated by at least two different cleavage mechanisms. One of the products had an observed mass of

11 430.1  $\pm$  6.6, which is consistent with the generation of a free carboxyl terminus or the corresponding amide (calculated mass 11 436.3 and 11 435.3, respectively). The other product had a mass of 11 407.8  $\pm$  4.2, which is consistent with decarboxylation and generation of a new carbonyl group at the C $\alpha$  of Ala102 (calculated mass 11 406.3). Hydroxyl radical cleavage of the peptide N–C $\alpha$  bond to generate an amide group was previously described for Ala–Ala incubated with EDTA–Fe in the presence of 2-mercaptoethanol (Hoyer et al., 1990) and for model peptide systems which mimic enzymatic amidation of biologically active peptides (Bateman et al., 1985). The hydrolytic cleavage of a peptide bond by an EDTA–Fe moiety attached to carbonic anhydrase was reported by Rana and Meares (1991). On the other hand, the generation of a carbonyl group at the C $\alpha$  of peptide bonds has been observed for a 16-residue peptide model modified with EPD–Fe and incubated with ascorbate (Platis et al., 1993). The same product was previously demonstrated for hydroxyl radical induced degradation of polyalanine after  $\gamma$ -radiolysis in the presence of oxygen (Garrison, 1987, and references therein). The cleavage reaction products, consistent with the generation of a carbonyl group at the C $\alpha$  of peptide bonds based on the mechanism proposed by Garrison (1987) for the degradation of polyalanine and by Platis et al. (1993) for the EPD-mediated cleavage of a peptide, are shown in Figure 9.

**Measuring Protein Oxidation Occurring during the Cleavage Reaction.** The standard cleavage reaction and reaction blank were carried out on H124C–EDTA–Fe. The number of carbonyl groups introduced during cleavage was measured spectrometrically after reaction with DNPH (see Experimental Procedures). The blank and reaction gave values of 0.06 and 0.26 mol of carbonyl/mol of protein, respectively. Thus 0.20 mol of carbonyl/mol of protein was introduced as a result of the cleavage conditions.

**Monitoring the Equilibrium Unfolding of H124C–EDTA–Fe by Quantitative Chemical Cleavage.** The cleavage technique will be of value in monitoring conformational equilibria such as the protein folding/unfolding reaction if the cleavage chemistry is fast compared to the rate constants for the conformational equilibrium. The chemical cleavage technique was used to follow the unfolding of H124C–EDTA–Fe at equilibrium as a function of GuHCl concentration in the presence and absence of Ca<sup>2+</sup> and pdTp to address its utility in quantitating the level of conformational states. The cleavage reaction can indeed be used quantitatively to monitor the unfolding of nuclease at equilibrium (Figure 10A). The unfolding transitions obtained by cleavage and fluorescence do not superpose in the region of denaturant concentration below  $C_m$  (Figure 10B). When this type of behavior is observed for two different optical probes, it is accepted as evidence of an equilibrium folding intermediate. In this case the cleavage chemistry could be affected by GuHCl; thus we investigated the equilibrium in the presence of the nuclease ligands Ca<sup>2+</sup> and pdTp. The addition of these ligands shifts the unfolding curve monitored by fluorescence (Figure 10B), because the native state is favored by mass action. The addition of Ca<sup>2+</sup> and pdTp shifts the unfolding curve monitored by chemical cleavage in a similar fashion. The ligand binding sites are well removed from the site of EPD attachment and the site of cleavage; thus this is not a direct steric effect. The cleavage yield in the absence of GuHCl is very similar with and without ligands; thus the

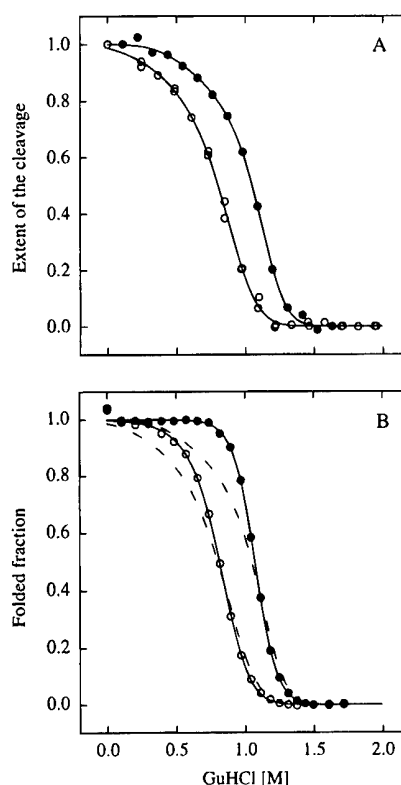


FIGURE 10: GuHCl-induced unfolding of H124C–EDTA–Fe as monitored by the yield of cleavage at residue 102 (A) and tryptophan fluorescence (B). Protein solutions were incubated with (●) and without (○) 10 mM Ca<sup>2+</sup> and 1 mM pdTp as described in Experimental Procedures prior to the cleavage reaction or the fluorescence measurement. The area under peak b (Figure 5C) was used to quantitate the yield of the cleavage reaction. Curves from (A) were overlaid (---) on (B) to compare the transition as seen by the two probes.

effect is not due to a change in the protein structure. This observation also indicates that the ligands do not serve to increase the cleavage reaction yield. At 0.3 M GuHCl, within the native baseline defined by fluorescence, the cleavage yield is reduced in the absence of ligands but not in their presence. It is unlikely that the ligands can ameliorate the putative chemical quenching effect due to GuHCl. Strong quenching agents such as mannitol and thiourea had little effect on the cleavage yield at 0.5 M concentration. Lower concentrations of GuHCl would not be expected to have such a direct quenching effect. If the decrease in cleavage yield were due to a direct interaction of GuHCl with the chelator, the low levels of Ca<sup>2+</sup> or pdTp added would not be sufficient to compete with the chelator for the high concentration of GuHCl. If GuHCl interacted with the chelator inhibiting hydroxyl radical formation, and the ligands competed with GuHCl for binding at the chelator, the ligands would have to interact with the chelator in such a way that they did not influence the production of oxygen radicals. Thus the deviation between the two probes (fluorescence and chemical cleavage) appears to be due to the presence of an equilibrium unfolding intermediate populated at low GuHCl concentrations.

**Conformational Analysis of the Nuclease–EDTA–Fe Adducts.** We hypothesized that backbone cleavage could occur when the  $\alpha$ -carbon site of oxidation is sufficiently solvent accessible and the iron ion is in close proximity to produce a sufficient concentration of oxygen radicals. A

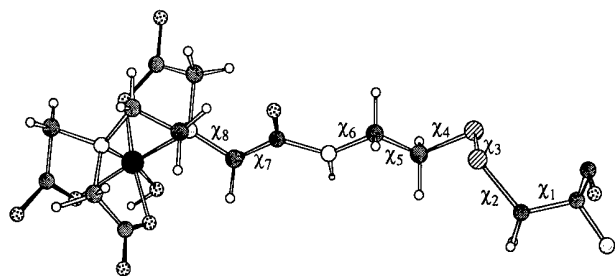


FIGURE 11: Structural model of an EPD-Fe-modified Cys residue. The conformational angles sampled are indicated for the Cys residue ( $\chi_1, \chi_2$ ) and for the reagent ( $\chi_3-\chi_8$ ), as described in Experimental Procedures.

conformational analysis of the EDTA-Fe reagent in the context of each nuclease cysteine variant was carried out as described in Experimental Procedures to test this hypothesis and to define a simple model to explain the observed cleavage patterns. The molecular model used in these calculations is shown in Figure 11. Internal van der Waals clashes between atoms of the reagent were determined initially, and only those conformations without overlaps were sampled in the context of the folded protein. Of 20 736 possible reagent conformations, 18 698 were free of internal van der Waals clashes. The cysteine sites were initially selected to be at the protein surface to minimize perturbation of the tertiary structure and thermodynamic stability of the nuclease variants. This surface exposure resulted in rejection of a relatively small fraction of the reagent conformations due to overlap with the protein structure (Table 3). The position of the Fe site for each allowed Cys-reagent conformation was recorded. The spatial distribution of Fe sites was contoured and is displayed along with a C $\alpha$  trace

in Figure 12. Cysteine sites C11 and C13 result in similar Fe distributions (Figure 12A). The C $\alpha$ -C $\beta$  vector of these sites projects in a similar direction as these residues are separated by one intervening residue (distance C $\alpha$ 11-C $\alpha$ 13 = 7.0 Å) on a  $\beta$ -strand. The common sites of cleavage observed occur below the overlapping Fe distributions. The calculated Fe distributions for K64C, K70C, and H124C are shown in Figure 12B. Each distribution covers a distinct region of the protein surface. The A102 site is cleaved in both K64C-EDTA-Fe (yellow) and H124C-EDTA-Fe (magenta). This site occurs between the two distributions. The contour plots provide a qualitative impression that the sites of cleavage are in close proximity to the Fe distribution derived from a conformational search of the reagent. To put this analysis on a quantitative footing, we calculated the radial distribution of Fe sites from each  $\alpha$ -carbon (Figure 13). The radial distribution functions are truncated at a 20-Å radius in the figures for clarity. No Fe positions were observed between 0 and 4 Å in any of the mutants analyzed because of van der Waals steric exclusion. The cleavage sites observed occur at sites where a fraction of conformers bring the Fe atom in close proximity to the C $\alpha$  position. The differences between the radial distribution functions of the cleavage reagent attached at different positions are determined by the path of the polypeptide as it traces toward and away from a particular attachment site (also see Figure 12). In each case a region including the site of reagent attachment is near the Fe distribution; frequently this region contains a local cleavage site.

No attempt has been made to determine the relative free energy of these conformations and thus their relative population. We have also not allowed for movement of either side

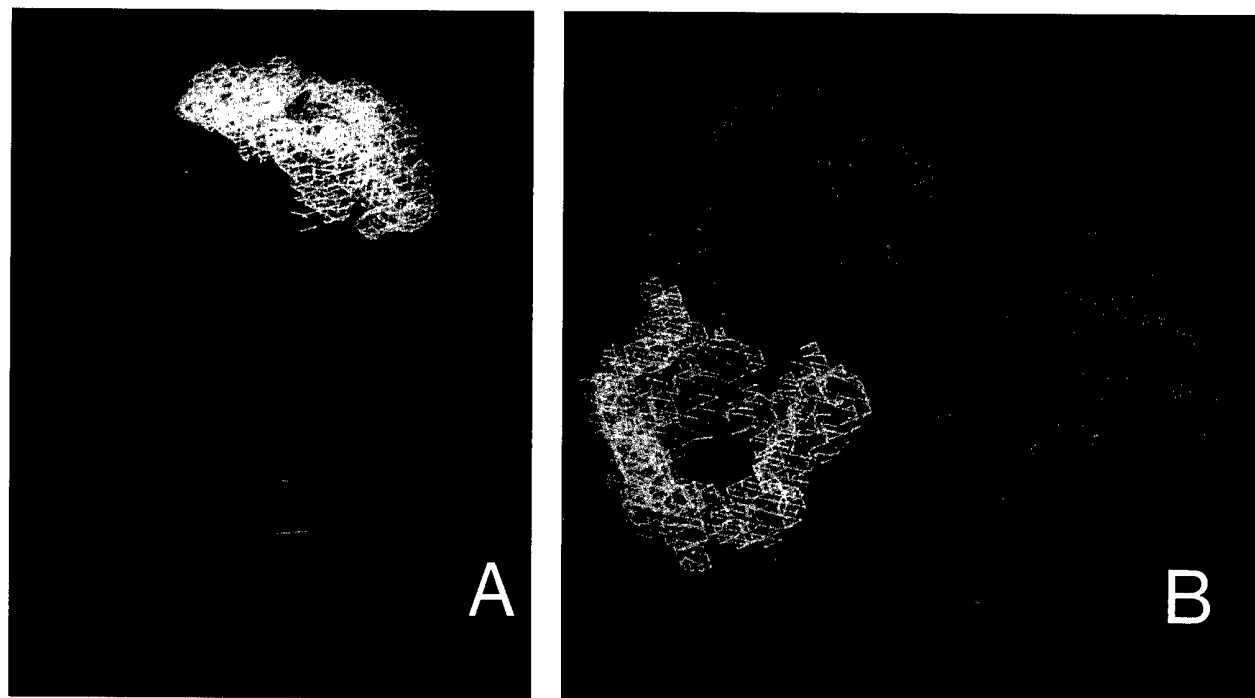


FIGURE 12: Conformational analysis of the nuclease-EDTA-Fe adducts. A model of the nuclease modified with EPD-Fe was used to sample low-energy rotamer conformations. Those with van der Waals overlap within the reagent or between the reagent and the protein were excluded. The Fe positions for the allowed conformers are included within the contours. (A) The distribution of Fe sites for P11C (magenta) and T13C (yellow) overlap, consistent with their common set of cleavage sites. (B) The Fe distribution for K64C (yellow), K70C (green), and H124C (magenta) is well separated on the protein surface, consistent with their distinct distributions of cleavage sites. Cleavage at A102 on the central  $\alpha$ -helix is observed with EPD-Fe cleavage of the K64C (yellow) and H124C (magenta) variants. Sites of cleavage are shown in red.

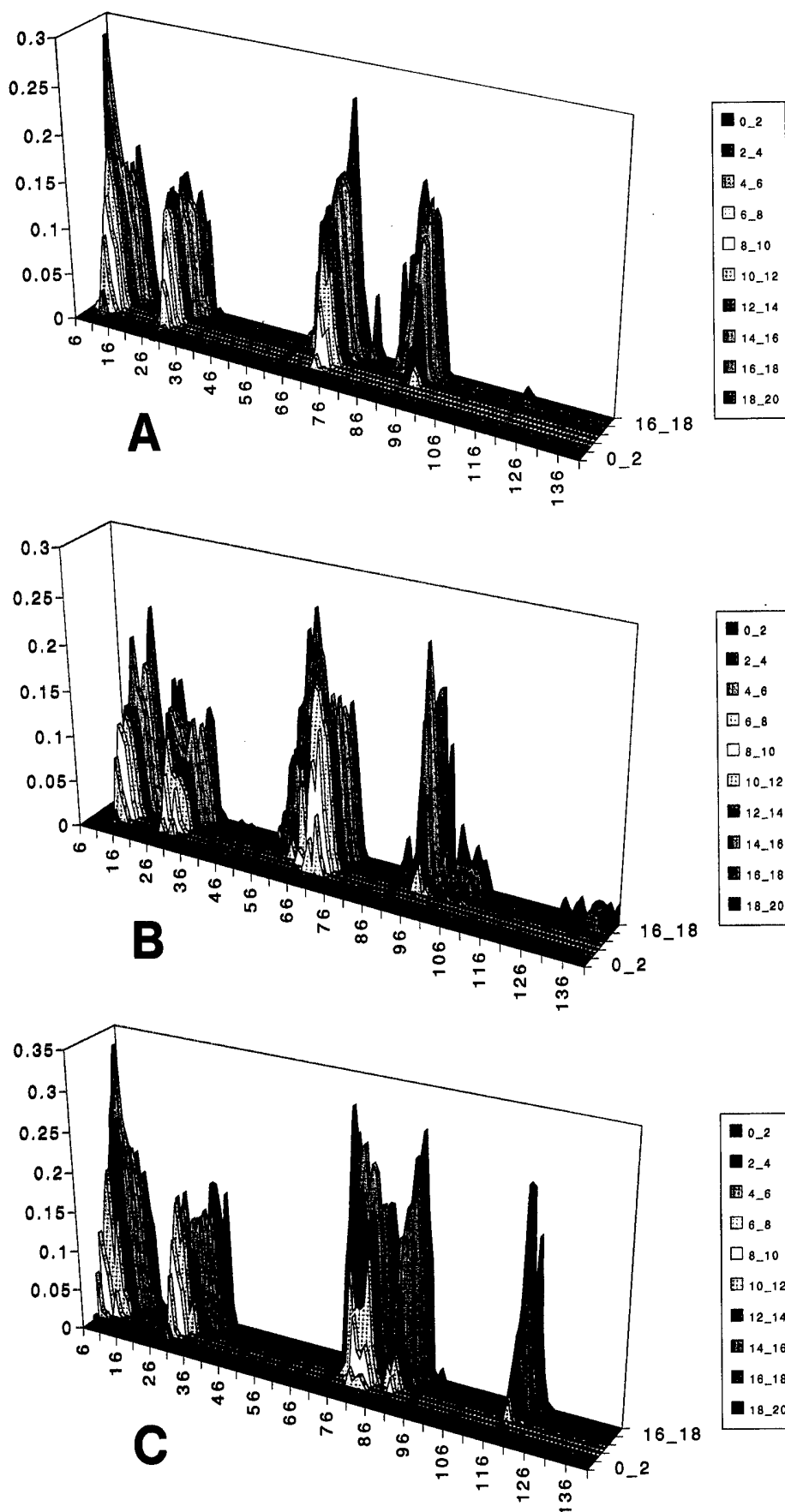
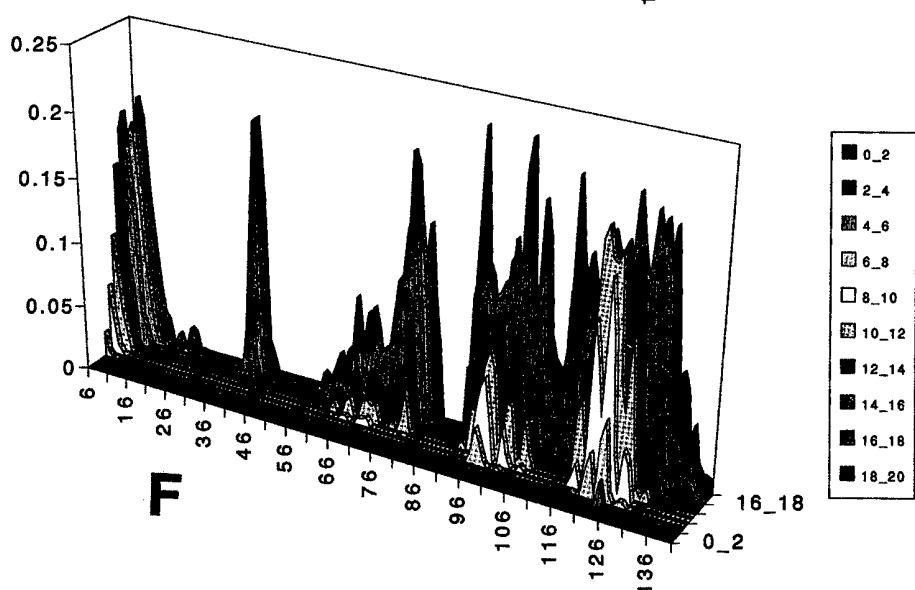
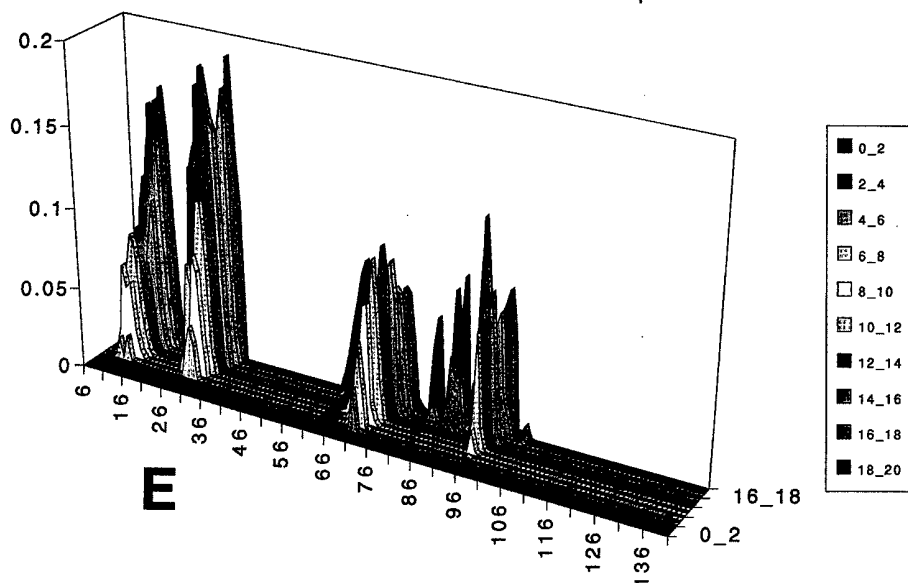
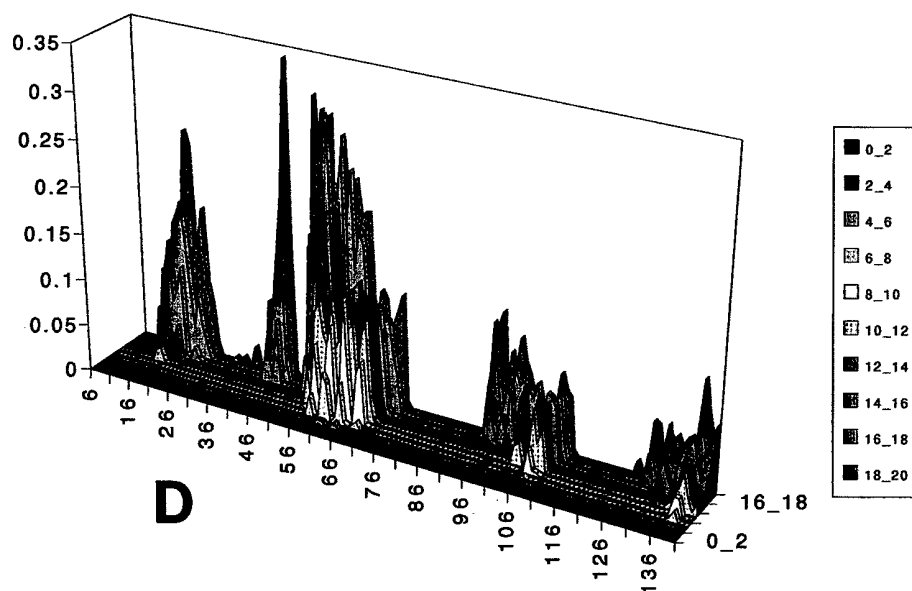


FIGURE 13: Radial distribution of Fe sites predicted from the conformational search. The amino acid sequence is plotted along the long axis. The fraction of Fe sites is plotted on the vertical axis, and the radius is plotted in 2-Å shells starting with the first nonzero shell (4–6 Å in orange) and ending with 18–20 Å in dark blue, projecting into the page. The radial distribution from a particular Ca to the population of predicted Fe sites is given by projecting the sequence number back through the color distribution of the plot. Note that the distribution



has been truncated at a 20-Å radius for clarity. The cleavage sites are indicated by the black lines on the base plane of the diagram. The distribution is provided for nuclease (A) P11C, (B) T13C, (C) K28C, (D) K64C, (E) K70C, and (F) H124C. The color coding of the radial shells is provided at the side of the figure.

chains or the protein backbone. Thus some reagent conformations may occur in the context of a conformationally dynamic protein that are excluded in our calculations. The conformational fluctuations of the protein about the equilibrium crystal structure also contribute to the uncertainty in the conformational analysis reported herein. We have assumed that the reagent does not make specific hydrogen bonds with the protein, limiting the conformational distribution from that calculated. The length and flexibility of the reagent tether would result in a high entropic penalty if the reagent were sequestered in a single conformation, generally making its localization unlikely. Further, multiple and distributed cleavage sites are observed for each modified nuclease variant that are most easily explained by multiple reagent conformations.

The conformational analysis provides a prediction of the region of the protein where cleavage would be expected when combined with the solvent accessibility calculations. There are additional solvent-accessible sites that would be predicted as sites of cleavage by the conformational and accessibility calculations that have not yet been identified by experiment. Such additional cleavage sites may be identified when lower concentrations of cleavage products can be characterized or they may not occur due to further complexities of the chemistry.

## DISCUSSION

The EPD-Fe reagent can be used to easily modify protein sulfhydryl groups with high yield. Only a modest perturbation to the structure, function, and thermodynamic stability of the protein molecule was observed when sites of cysteine substitution (and subsequent modification) were selected on the protein surface. Initiation of the cleavage reaction on addition of the iron reductant ascorbate leads to a distinct fragmentation pattern of the polypeptide backbone for each of the nuclease cysteine variants examined. Under the conditions used for this study, the cleavage reaction occurs within the nuclease adduct generating the hydroxy radical, as the attachment of the reagent is required to yield protein cleavage (Ermácora et al., 1992).

The cleavage yield is relatively low (1–15%) but sufficient for chemical characterization of the cleavage products. Previous characterization of the cleavage products of an EPD-Fe-modified peptide (Platis et al., 1993) indicated that the disulfide linkage is more sensitive to oxidative cleavage than the polypeptide backbone. The reagent was also found to undergo oxidative damage. These observations may explain the limited yield observed for the nuclease cysteine variants examined in this and previous studies (Ermácora et al., 1992). Only a limited number of cleavage sites are observed for each cysteine variant. This is consistent with the low fraction of C $\alpha$  atoms that are exposed on the surface of this globular protein. Relatively few cleavage sites are observed close in sequence to the site of attachment. This may be due to the lack of surface exposure of neighboring C $\alpha$  atoms at adjacent sites. The conformational flexibility and intramolecular steric exclusion may also serve to make localization of the reagent at the attachment site a relatively rare event. The H124C variant does show local cleavage in the denatured state, and extensive local cleavage was observed in the model peptide study of Platis et al. (1993).

The fragile nature of the disulfide linkage and the lack of protein cleavage by free EDTA-Fe (Ermácora et al., 1992)

at concentrations equimolar to the protein combine to make protein backbone cleavage a relatively rare event. This is an advantage in studying protein systems where the cleavage of a native protein molecule will result in unfolded fragments. In the case of EPD-Fe cleavage, the system is designed to favor a single-hit reaction before the reagent is removed from the protein or destroyed. This helps to ensure that the cleavage products observed are derived from the protein state of interest, rather than from continued cleavage of a protein fragment in a different conformational state.

The cleavage reaction will yield products under a wide range of conditions and in the presence of an array of solutes. Significant yields were observed over a pH range of 4–9. The low pH extreme allows the reagent to be used in the examination of the molten globule state of proteins such as apomyoglobin that are populated under acidic conditions (Barrick & Baldwin, 1993). Unfortunately, the reagent does not mediate cleavage at pH = 2.0 when some A-states are populated. Presumably, at very low pH, the carboxylate groups become protonated and the iron ion is not retained in an EPD complex. The cleavage reaction can also be carried out in the presence of denaturants and over a range of temperatures, allowing both native and nonnative states to be examined with this technique. Significant cleavage occurs within 5–30 min. The reaction can be accelerated significantly with the addition of 10 mM H<sub>2</sub>O<sub>2</sub>. In the absence of peroxide the reaction is dependent on molecular oxygen (Ermácora et al., 1992).

Polypeptide cleavage is observed at residues close in sequence to the site of attachment as well as at sites distant in sequence but brought close to the reagent by the protein fold. The yield of cleavage products due to long-range cleavage is dramatically reduced or eliminated in the presence of denaturant, supporting the conclusion that the cleavage products monitor the folded state of the protein. A modest level of cleavage product was observed for the P11C variant when the cleavage was carried out in 4.8 M urea (Figure 4A, lane 4, 14-kDa band) that was identified as resulting from cleavage at K28 and G29 in the native cleavage reaction. These products monitor the proximity of  $\beta$ -strand 1 to the  $\beta$ -turn connecting  $\beta$ -strands 2 and 3 in an antiparallel three-stranded  $\beta$ -meander in the native structure of the protein. The persistence of this band is consistent with the previous proposal that the  $\beta$ -sheet of nuclease may persist to some degree in urea (Shortle & Meeker, 1989; Flanagan et al., 1992). Interestingly, the N-terminal  $\beta$ -meander is part of the early folding intermediate identified by pulsed amide exchange and NMR (Jacobs & Fox, 1994).

Chemical cleavage of the cysteine variants examined provides proximity information for pairs of secondary structural elements. The K64C (helix 1) variant yields cleavage in helix 2 (Ala102). Likewise H124C in helix 3 cleaves within helix 2. Both results are consistent with the proximity of these helical elements in the structure of the protein (Figure 6D,F). The P11C and T13C ( $\beta$ -strand 1) variants both yield cleavage within the  $\beta$ -turn connecting  $\beta$ -strands 2 and 3 (Lys28 and Gly29) and thus identify sites within the antiparallel three-stranded  $\beta$ -meander at the N-terminus of the protein (Figure 6A,B). The K70C variant appears to yield some long-range cleavage sites (Figure 3A) which were not mapped due to their low yield. The K28C variant reported previously (Ermácora et al., 1992) provides information concerning the proximity of the  $\beta$ -strands 2 and

3 and the long loop connecting  $\beta$ -strands 4 and 5, and thus the integrity of the twisted  $\beta$ -sheet. Thus the cleavage sites provide probes for the presence of specific substructures within the protein and indeed have already been effective in identifying a new equilibrium folding intermediate. These probes should also be of value in investigations of nonnative states of the protein.

Large fragments of nuclease (residues 1–136 of 149; nuclease  $\Delta$  137–149) have been prepared, with properties similar to those of the molten globule state of other proteins and intermediate between the native and unfolded states of nuclease (Flanagan et al., 1992; Shortle & Meeker, 1989). The chemical cleavage sites mapped for this series of cysteine variants in the native state provide proximity information for various pairs of secondary structure elements as described above. These cysteine variants should be useful in identifying residual elements of native-like structure in the nuclease fragments.

A significant fraction of EPD-mediated polypeptide cleavage occurs via at least two oxidative mechanisms (Platis et al., 1993) and a hydrolytic mechanism (Rana & Meares, 1991). The oxidative mechanisms may be mediated by diffusible hydroxyl radicals or by an iron-bound oxygen radical brought to the protein surface by the flexible reagent tether. The data and calculations presented herein do not discriminate between these two alternatives, and indeed both may be involved in the observed backbone cleavage. In either case the lifetime of the reactive oxygen species must be short compared to the lifetime of the protein conformational state as discussed below.

*Monitoring the Equilibrium Unfolding of H124C–EDTA–Fe by Quantitative Chemical Cleavage.* The unfolding curves based on fluorescence and chemical cleavage do not superpose at GuHCl concentrations below  $C_m$ . The addition of ligands results in a comparable shift of these unfolding curves to higher  $C_m$  without affecting their shape. Thus it appears that a native-like intermediate exists with a  $C_m$  significantly below that observed by fluorescence, which monitors the global unfolding of the protein. The Trp140 environment, monitored by fluorescence, does not change significantly during the transition at low GuHCl. The intermediate must be very much like the native protein because the Trp140 environment is composed of segments well separated in protein sequence. The H124C site is near the N-terminus of helix 3 while Trp140 is in a loop following helix 3.

The chemical cleavage event monitored is at Ala102 in helix 2. The H124C site follows a type VI $\alpha$   $\beta$ -turn (residues 115–118) containing a *cis* K116–P117 peptide bond that is in equilibrium with the *trans* configuration which is a native-like folding intermediate of the protein structure (Nakano et al., 1993; Chen et al., 1992; Evans et al., 1989; Alexandrescu et al., 1989). This region is under strain and is thus a good candidate for local unfolding prior to the global unfolding transition (Hodel et al., 1993). Thus the decrease in cleavage yield at low GuHCl concentrations may be due to a local unfolding of nuclease in the region containing the H124C site of attachment.

At GuHCl concentrations above  $C_m$  the chemical cleavage and fluorescence curves superpose. Thus the chemical cleavage technique using the EPD reagent provides a faithful measure of the folded protein concentration. This indicates that the lifetime of reactive oxygen species involved must

be much shorter than the lifetime of the native and unfolded states. If the lifetime of the reactive oxygen species were long compared to the folding times, an overestimate of the folded material would result and the curves would be shifted to higher denaturant concentrations. These results are consistent with the mechanism based on highly reactive and short-lived hydroxyl radicals inferred from the nature of the cleavage products observed by Platis et al. (1993) for an EPD-modified peptide and the cleavage products reported herein. The cleavage products observed for the tricarboxylate EPD reagent are distinct from those reported using the related tetracarboxylate BABE reagent (Rana & Meares, 1991). In the latter case, a stable iron peroxy species is proposed to carry out a hydrolytic cleavage of peptide bonds. The lifetime of such a species may be comparable to or longer than those of the native and unfolded states. If this were the case, use of the tetracarboxylate class of reagents could lead to erroneous estimates of folding equilibria.

*Conformational Analysis of EDTA–Fe–Protein Adducts.* The observed cleavage sites have significant accessibility to solvent or are on the surface of the protein where modest motion of the protein or its side chains would yield access to diffusible or Fe-bound reactive oxygen species. The lack of internal sites may be due to the high reactivity of hydroxyl radicals compared with its diffusion rate into the protein or the Fe-bound nature of some reactive oxygen species. The chemical cleavage approach thus allows the surface of the protein to be explored over a modest region of the protein exterior. The length of the reagent tether, its intrinsic flexibility when attached to surface residues, and the diffusion of free radicals from their site of generation may all contribute to the range of observed cleavage sites. The combination of solvent accessibility and proximity to the distribution of iron positions predicted from the conformational search is sufficient criteria to predict the observed cleavage sites. Other potential cleavage sites would also be predicted from these calculations that have not been characterized. These may occur at a lesser yield and would thus have not been detected in the present analysis.

Alternatively, other factors may be involved that were not anticipated by the simple conformational analysis reported herein. The conformational search calculation should be useful in anticipating sites or regions of cleavage in a protein of known structure and should thus facilitate the design of new experiments. The protein cleavage technique will be most powerful when used to compare the cleavage pattern observed by a protein molecule under two sets of conditions, such as the native and a nonnative state, where the maintenance, gain, or loss of specific cleavage sites can be monitored.

*Uses and Limitations for the Study of Unknown Structures.* The chemical cleavage method provides a complementary approach to NMR spectroscopy in the investigation of nonnative states of proteins. Some proteins in the molten globule or other nonnative states aggregate or yield broad resonances due to conformational fluctuations with intermediate exchange rates, making them unsuitable for NMR spectroscopy. When a suitable sample can be prepared, the chemical shift dispersion of resonances from their random coil values is modest, leading to complications in assignment and interpretation of NOE data. NOE-derived short-range distances can be combined to yield the structure of proteins in the native state where a well-defined conformation exists.

Nonnative states of proteins may exist as a dynamic population of structures, with short-range NOE's observed from distinct conformers that may not occur simultaneously in a single structure. There is no method to identify this problem other than the structural incompatibility of the observed distances. Overinterpretation of NOE-derived distances observed for dynamic systems could lead to erroneous proposals of structure in nonnative states.

The distances mapped by the chemical cleavage method (10–15 Å) are longer than those monitored by NMR (<5 Å), allowing the proximity of secondary structural elements to be inferred from the cleavage pattern. The cleavage pattern is also dependent on conformation and identifies residues on the surface of the protein molecule. The relatively small number of sites that can be identified and the softness of the distance estimates will obviously preclude the independent identification of the protein conformation but will allow comparisons of the native and a nonnative states of the protein. The identification of long-range proximity of two residues in a nonnative state will also serve to validate the structure of nonnative protein states inferred from many short-range interactions when they can be observed under similar conditions with NMR spectroscopy.

The chemical cleavage technique could also be of value in testing proposals for the protein fold for a molecule of unknown structure. A series of cysteine variants could be prepared and cleavage sites identified as reported herein. The resulting cleavage data would provide information concerning the general proximity of residue pairs and the surface exposure of cleavage sites. This information should be sufficient to discriminate among several models for the three-dimensional structure of the protein.

Protein side chains are also oxidized by EDTA-Fe-mediated oxygen radical production (Stadtman, 1992). The reactivity of side chains varies with the chemical nature, making their oxidation a less general monitor of surface accessibility. Extensive side-chain oxidation could alter the stability and structure of a protein, particularly when in a marginally stable nonnative state, compromising the usefulness of the methods reported herein. Fortunately, the extent of side-chain plus backbone oxidation is quite low as described above. Oxidative peptide cleavage which introduces a carbonyl group at the site of cleavage has been identified in this and other protein oxidation systems (Hoyer et al., 1990; Platis et al., 1993). Thus a fraction of the carbonyl groups measured in this study must result from a cleavage event and not side-chain modification. In any event, our values for protein oxidation and cleavage are lower than that observed in other metal-catalyzed oxidation systems (Levine et al., 1994; Ue et al., 1992; Kulmacz et al., 1994; Soundar & Coleman, 1993). These differences are likely due to the inherently fragile nature of the EPD-protein conjugates discussed above. The low level of potential side-chain oxidation and backbone cleavage ensures that the majority of the observed backbone cleavage will occur in unoxidized protein molecules. Thus side-chain oxidation should not compromise the interpretation of cleavage data. With the implementation of more advanced mass spectral techniques such as tandem mass spectrometry, identification of side-chain oxidation sites will provide additional topological information for the proteins under investigation and thereby

increase the utility of this technique for the study of both native and nonnative protein states.

#### *Uses of Fe<sup>2+</sup>-Mediated Protein Oxidation and Cleavage.*

Fe-mediated protein oxidation and cleavage has been of value in structural studies beyond the use of protein modification reagents such as EPD-Fe described herein and in earlier studies reported by Rana and Meares (1991) concerning a related EDTA-Fe-based reagent. Ue et al. (1992) have used Fe<sup>2+</sup>-mediated cleavage to map the metal binding site of actin. The active site of pig heart NADP-specific isocitrate dehydrogenase was identified by affinity cleavage with Fe<sup>2+</sup> isocitrate (Soundar & Coleman, 1993). The Fe<sup>2+</sup> site of glutamine synthetase has been identified by oxidation and protein cleavage (Jhon et al., 1991; Climent & Levine, 1991). The low chemical selectivity observed in such systems should make this class of experiments valuable in related and new applications.

## CONCLUSIONS

The chemical cleavage technique identifies solvent-accessible residues on the surface of the protein within a radius of approximately 15 Å from the cysteine attachment sites. Thus the technique is useful in monitoring the proximity of adjacent secondary structural elements and the integrity of the tertiary fold of the protein. The technique is capable of monitoring the relative fraction of native and denatured states and should thus provide a realistic view of the nonnative protein structures. This result implies that the kinetics of cleavage are rapid compared to those for protein folding. The cleavage technique has identified the presence of an equilibrium folding intermediate at low denaturant concentrations. Thus the method should be of value in monitoring the structure of nonnative states such as the molten globule by comparison of cleavage patterns under native and nonnative conditions.

## ACKNOWLEDGMENT

We thank the Yale University School of Medicine, Protein and Nucleic Acid Chemistry Facility, for amino acid analysis and peptide sequencing. We thank Fred Richards for helpful discussions and Isobel Parsons, Alan Robertson, and Alex Golden for technical assistance.

## REFERENCES

- Alexandrescu, A. T., Ulrich, E. L., & Markley, J. L. (1989) *Biochemistry* 28, 204–211.
- Barrick, D., & Baldwin, R. L. (1993) *Biochemistry* 32, 3790–3796.
- Bateman, R. C., Jr., Youngblood, W. W., Busby, W. H., Jr., & Kizer, J. S. (1985) *J. Biol. Chem.* 260, 9088–9091.
- Chen, H. M., Markin, V. S., & Tsong, T. Y. (1992) *Biochemistry* 31, 1483–1491.
- Climent, I., & Levine, R. L. (1991) *Arch. Biochem. Biophys.* 289, 371–375.
- Cuatrecasas, P., Fuchs, S., & Anfinsen, C. B. (1967) *J. Biol. Chem.* 242, 1541–1547.
- Eftink, M. R., Ghiron, C. A., Kautz, R. A., & Fox, R. O. (1991) *Biochemistry* 30, 1193–1199.
- Ellman, G. L. (1959) *Arch. Biochem. Biophys.* 82, 70–77.
- Ermácora, M. R., Delfino, J. M., Cuenoud, B., Schepartz, A., & Fox, R. O. (1992) *Proc. Natl. Acad. Sci. U.S.A.* 89, 6383–6387.

- Evans, P. A., Kautz, R. A., Fox, R. O., & Dobson, C. M. (1989) *Biochemistry* 28, 362–370.
- Flanagan, J. M., Mikio, K., Shortle, D., & Engelman, D. M. (1992) *Proc. Natl. Acad. Sci. U.S.A.* 89, 748–752.
- Garrison, W. M. (1987) *Chem. Rev.* 87, 381–398.
- Goto, Y., Nobuaki, T., & Fink, A. L. (1990) *Biochemistry* 29, 3480–3488.
- Hellings, H. W., & Richards, F. M. (1991) *J. Mol. Biol.* 222, 763–785.
- Hertzberg, R. P., & Dervan, P. B. (1984) *Biochemistry* 23, 3934–3945.
- Hodel, A., Kautz, R. A., Jacobs, M. S., & Fox, R. O. (1993) *Protein Sci.* 2, 838–850.
- Hoyer, D., Cho, H., & Schultz, P. G. (1990) *J. Am. Chem. Soc.* 112, 3249–3250.
- Hynes, T. R., & Fox, R. O. (1991) *Proteins: Struct., Funct., Genet.* 10, 92–105.
- Hynes, T. R., Kautz, R. A., Goodman, M. A., Gill, J. F., & Fox, R. O. (1989) *Nature* 339, 73–76.
- Jacobs M., & Fox, R. O. (1994) *Proc. Natl. Acad. Sci. U.S.A.* 91, 449–453.
- Jennings, P. A., & Wright, P. E. (1993) *Science* 262, 892–896.
- Jhon, D. Y., Kim, K., & Byun, S. M. (1991) *Biofactors* 3, 121–125.
- Kim, K., Rhee, S. G., & Stadtman, E. R. (1985) *J. Biol. Chem.* 260, 15394–15397.
- Kulmacz, R. J., Palmer, G., Wei, C., & Tsai, A. (1994) *Biochemistry* 33, 5428–5439.
- Lee, B., & Richards, F. M. (1971) *J. Mol. Biol.* 55, 379–400.
- Levine, R. L., Williams, J. A., Stadtman, E. R., & Shacter E. (1994) *Methods Enzymol.* 233, 346–357.
- Mach, H., Ryan, J. A., Burke, C. J., Volkin D. B., & Middaugh, C. R. (1993) *Biochemistry* 32, 7703–7711.
- Matsudaira, P. (1987) *J. Biol. Chem.* 262, 10035–10038.
- Matthews, C. R. (1993) *Annu. Rev. Biochem.* 62, 653–683.
- Nakano, T., Antonino, L. C., Fox, R. O., & Fink, A. L. (1993) *Biochemistry* 32, 2534–2541.
- Nozaki, Y. (1972) *Methods Enzymol.* 26, 43–50.
- Penefsky, H. S. (1979) *Methods Enzymol.* 56, 527–530.
- Platis, I. E., Ermácora, M. R., & Fox, R. O. (1993) *Biochemistry* 32, 12761–12767.
- Rana, T. M., & Meares, C. F. (1991) *Proc. Natl. Acad. Sci. U.S.A.* 88, 10578–10582.
- Schägger, H., & von Jagow, G. (1987) *Anal. Biochem.* 166, 368–379.
- Shortle, D., & Meeker, A. K. (1989) *Biochemistry* 28, 936–944.
- Soundar, S., & Colman, R. F. (1993) *J. Biol. Chem.* 268, 5264–5271.
- Stadtman, E. R. (1992) *Science* 257, 1220–1224.
- Taniuchi, H., & Anfinsen, C. B. (1966) *J. Biol. Chem.* 241, 4366–4385.
- Timasheff, S. N., & Arakawa, T. (1989) in *Protein Structure. A Practical Approach* (Creighton, T. E., Ed.) pp 331–345, IRL Press, Oxford, England.
- Ue, K., Muhrad, A., Edmonds, C. G., Bivin, D., Clark, A., Piechowski, W. V., & Morales, M. F. (1992) *Eur. J. Biochem.* 203, 493–498.
- Wolff, S. P., Garner, A., & Dean, R. T. (1986) *Trends Biochem. Sci.* 11, 27–31.